Title

Evolution of metal hyperaccumulation required *cis*-regulatory changes and triplication of *HMA4*

Marc Hanikenne[*,1,†], Ina N. Talke[*,1,§], Michael J. Haydon[1,§], Christa Lanz[2], Andrea Nolte[1,‡], Patrick Motte[3,4], Jürgen Kroymann[5], Detlef Weigel[2], Ute Krämer[1,§]

[*]These authors contributed equally. [1]Max Planck Institute of Molecular Plant Physiology, D-14476 Potsdam, Germany. [2]Max Planck Institute for Developmental Biology, D-72076 Tübingen, Germany. [3]Plant Cell Biology, Dept. of Life Sciences, University of Liège, B-4000 Liège, Belgium. [4]Center for Assistance in Technology of Microscopy, Dept. of Chemistry, University of Liège, B-4000 Liège, Belgium.[5]Max Planck Institute for Chemical Ecology, D-07745 Jena, Germany. [†]Present address: [3]. [‡]Present address: Department of Thoracic, Cardiac and Vascular Surgery, University of Tübingen, D-72076 Tübingen, Germany. [§]Present address: BIOQUANT Center, Heidelberg Institute of Plant Sciences, University of Heidelberg, D-69120 Heidelberg, Germany.

SUMMARY

Little is known about the types of mutations underlying the evolution of species-specific traits. The metal hyperaccumulator *Arabidopsis halleri* has the rare ability to colonize heavy metal-polluted soils, and, as an extremophile sister species of *Arabidopsis thaliana*, it is a powerful model for research on adaptation[1-3]. *A. halleri* naturally accumulates and tolerates leaf concentrations as high as 2.2% zinc and 0.28% cadmium in dry biomass[4]. Based on transcriptomics studies, metal hyperaccumulation in *A. halleri* has been associated with more than 30 candidate genes, which are expressed at higher levels in *A. halleri* than in *A. thaliana*[4-6]. Some of these genes have been genetically mapped to broad chromosomal segments of between 4 and 24 cM co-segregating with Zn and Cd hypertolerance[7-9]. However, the *in planta* loss-of-function approaches required to demonstrate the contribution of a given candidate gene to metal hyperaccumulation or hypertolerance have not been pursued to date. Using RNA interference to downregulate *HMA4* expression, we show here that Zn hyperaccumulation and full hypertolerance to Cd and Zn in *A. halleri* depend on the metal pump HMA4. Contrary to a postulated global *trans* regulatory factor governing high expression of numerous metal hyperaccumulation genes, we demonstrate that enhanced expression of *AhHMA4* in *A. halleri* is attributable to a combination of modified *cis*-regulatory sequences and copy number expansion, in comparison to *A. thaliana*. Transfer of an *AhHMA4* gene to *A. thaliana* recapitulates Zn partitioning into xylem vessels and the constitutive transcriptional upregulation of Zn deficiency response genes characteristic of Zn hyperaccumulators. Our results demonstrate the importance of *cis*-regulatory mutations and gene copy number expansion in the evolution of a complex naturally selected extreme trait[10] (Supplementary Fig. 1). The elucidation of a natural strategy for metal hyperaccumulation is seminal for the rational design of technologies for the clean-up of metal-contaminated soils and for bio-fortification.

MANUSCRIPT TEXT

Heavy Metal ATPase 4 (*HMA4*)[4] is among a large number of genes more highly expressed in *A. halleri* than in *A. thaliana*[5,6] and encodes a plasma membrane protein of the 1_B family of transition metal pumps in the P-type ATPase superfamily[8,11]. To investigate whether *AhHMA4* functions in metal hyperaccumulation or hypertolerance of *A. halleri*, we reduced the expression of *AhHMA4* by RNA interference (RNAi)[12]. For this, we developed a genetic transformation system, which has not so far been available for hyperaccumulator species. *HMA4* transcript levels were decreased to between 45 and 10% of wild-type levels in different RNAi lines (Fig. 1a, Supplementary Fig. 2), which appeared morphologically normal. After cultivation of *HMA4* RNAi lines in hydroponic solutions, their shoots contained only 12 to 35% of Zn, compared to wild-type *A. halleri* (Fig. 1b, Supplementary Fig. 3). These levels were similar to shoot Zn concentrations in *A. thaliana* as a representative non-accumulator[4]. In roots of wild-type *A. halleri*, metal concentrations are low, reflecting high root-to-shoot metal fluxes[4,13,14]. By comparison, roots of *HMA4* RNAi lines accumulated 49- to 134-fold higher Zn concentrations, again similar to the non-accumulator *A. thaliana* (Fig. 1c). Partitioning and accumulation of metals other than Zn and Cd (Supplementary Fig. 4) were not consistently changed in *HMA4* RNAi lines. Together these results demonstrate that high *HMA4* transcript levels are required for highly efficient root-to-shoot Zn flux and for Zn hyperaccumulation in the shoots of *A. halleri*. This is distinct from the function of *A. thaliana HMA4* in root-to-shoot translocation of Zn for the maintenance of Zn-dependent processes in the shoot[15,16].

We next examined how *HMA4* alters the distribution of Zn within the roots of *A. halleri*, by imaging with the fluorescent Zn indicator Zinpyr-1[16]. In the wild type,

fluorescence was most intense in the xylem vessels located inwards from the pericycle cell layer of the root vasculature (Fig. 1d, Supplementary Fig. 5). By contrast, in the *HMA4* RNAi lines signal intensity was maximal in the pericycle cell layer, qualitatively similar to the change in Zn localization reported for the *A. thaliana hma4* mutant compared to the wild type[15]. This indicates that silencing of *A. halleri HMA4* impairs the release of Zn from the root symplasm into the apoplastic xylem vessels, which provide the primary pathway for the movement of solutes from the root to the shoot with the transpiration stream[17]. These results are in agreement with the decreased Zn partitioning into the shoots in *HMA4* RNAi lines.

If increased *HMA4* activity is a primary event in heavy metal hyperaccumulation, we would expect that this affects other candidate genes for hyperaccumulation known to be highly expressed in *A. halleri*[4]. We therefore analysed RNA from plants cultivated in a 5 µM Zn solution by real-time RT-PCR. Expression of Zn deficiency response genes[4,18] was specifically decreased in roots of the *HMA4* RNAi lines. For example, relative transcript levels of *IRT3* (Fig. 1e) and *ZIP4* (Fig. 1f) were correlated with *HMA4* transcript levels across all genotypes (r = 0.99 and 0.98, respectively). The membrane transporters encoded by *IRT3* and *ZIP4* are both members of the same family of proteins implicated in the cellular uptake of Zn[18]. Thus, the high expression of these genes in roots of wild-type *A. halleri*[4] appears to be a secondary consequence of increased *HMA4* activity, and is likely to further enhance shoot metal accumulation.

Heterologous expression of *AhHMA4* in cells of the budding yeast *Saccharomyces cerevisiae* was reported to confer metal tolerance[4] and metal hypersensitivity[8]. Recently, three respective major QTL for Zn and Cd hypertolerance were mapped in progeny from a cross between *A. halleri* and its metal-sensitive non-accumulator relative *A.*

lyrata[8,9]. Notably, major QTL for both Zn and Cd hypertolerance contained *HMA4*, but comprised several centiMorgans and thus at least several hundred genes. To examine whether *HMA4* functions not only in metal hyperaccumulation of *A. halleri*, but also in hypertolerance, we determined the effects of toxic metal concentrations on root growth of plants in hydroponic solutions[19,20]. In the presence of 30 µM Cd or 1.5 mM Zn, root elongation in wild-type *A. halleri* plants was still about 68% and 60% of the elongation under control conditions, respectively. In contrast, roots of *HMA4* RNAi lines exhibited only 3 to 15% and 12 to 37% of the elongation under control conditions, respectively (Fig. 1 g, h). These data demonstrate that *HMA4* makes a substantial contribution to Cd and Zn hypertolerance in *A. halleri*.

Our results indicate that *HMA4* has a key role in several aspects of the complex metal hyperaccumulator phenotype. We therefore addressed the molecular basis for elevated *HMA4* expression in *A. halleri* compared to the non-accumulator *A. thaliana*. Earlier, Southern blot screening provided circumstantial evidence that there may be more than a single *HMA4* gene copy in the genome of *A. halleri*[4]. However, information on the number of gene copies, their respective sequences, expression and functionality has been unavailable. To examine this, two overlapping *A. halleri* genomic BAC clones were sequenced. Compared to the syntenic segment in *A. thaliana*, there is a complex triplication of a region that includes *HMA4* (corresponding to At2g19110 in *A. thaliana*) and the two downstream genes (At2g19120 and At2g19130) (Fig. 2a). In addition to partial deletions and inversions of At2g19120 and At2g19130 orthologs, several transposon and retrotransposon insertions are evident. The flanking sequences are largely syntenic with *A. thaliana*. Within coding sequences, the three *AhHMA4* gene copies are on average 99% identical to each other, but share only 88% sequence identity

with *AtHMA4*, suggesting that the triplication may have occurred relatively recently in the *A. halleri* lineage (Supplementary Table 1). We specifically quantified either the *HMA4-1* cDNA alone or both the almost identical *HMA4-2* and *HMA4-3* cDNAs by real-time RT-PCR (Supplementary Fig. 6). The results are consistent with similar expression levels of all three *HMA4* gene copies (Fig. 2b). Thus, both an increase in copy number and elevated expression of individual gene copies contribute to the high transcript levels of *HMA4* in *A. halleri* in comparison with *A. thaliana*.

Sequence divergence from *A. thaliana* is most pronounced in the 5'-flanking regions of *A. halleri HMA4* genes (Supplementary Table 1)[21], suggesting possible regulatory innovations in *A. halleri*. To determine experimentally whether the increased expression of individual *HMA4* gene copies is due to *cis*-regulatory changes, we generated fusions of the promoters of *AtHMA4* and of the three *AhHMA4* gene copies to the *β-glucuronidase* (*GUS*) reporter for the transformation of both *A. halleri* and *A. thaliana*. Reporter activity directed by the *AtHMA4* promoter was much lower than that directed by any of the three *AhHMA4* promoters, which were as effective as the strong constitutive cauliflower mosaic virus (CaMV) 35S promoter (Fig. 3a-d). Spatial patterns of reporter activity for all three $AhHMA4_P$ constructs were highly similar in both *A. halleri* and *A. thaliana* (Supplementary Figs 7 to 10). Qualitatively, activity patterns were also similar for promoters originating from both species (Fig. 3e, g, Supplementary Figs 7, 8)[15]. The *HMA4* expression pattern was confirmed by *in situ* hybridization in wild-type *A. halleri* (Supplementary Figs 9, 10). This revealed specific mRNA accumulation in the root pericycle and xylem parenchyma (Fig. 3f, h, Supplementary Fig. 10), supporting a function of *HMA4* in xylem loading of Zn (see Fig. 1d). Expression in the xylem parenchyma and the cambium of leaves

(Supplementary Fig. 9) is consistent with a possible role of *HMA4* in metal distribution within the leaf blade and the exclusion of metals from specific cell types. Together, our data confirm that high *HMA4* transcript levels in *A. halleri* are the result of gene copy number triplication combined with the enhanced expression of all three *A. halleri HMA4* genes specified in *cis*.

Finally, we determined whether increased *HMA4* activity is not only necessary, but also sufficient for altered heavy metal accumulation and tolerance. To this end, we transformed *A. thaliana* with an *AhHMA4* mini-gene, consisting of an *AhHMA4* cDNA linked to the *AhHMA4-1* promoter. Primary transformants contained moderately elevated *HMA4* transcript levels (2.44 ± 0.08 and 2.85 ± 0.89 fold in roots and shoots, respectively, compared to wild type, mean ± s.e.m., $n = 6$; Supplementary Fig. 9m-o), at the lower end of the range expected based on previous comparisons between *A. halleri* and *A. thaliana*[4]. Zinpyr-1 imaging showed high levels of Zn in xylem tissues of roots of transgenic plants (Fig. 4a), mimicking the distribution of Zn in wild-type *A. halleri* (see Fig. 1d). By contrast, in non-transgenic *A. thaliana* Zn levels were highest in the root pericycle cell layer (Fig. 4a), resembling the localization in *A. halleri HMA4* RNAi lines (see Fig. 1d). Thus, transformation of *A. thaliana* with *AhHMA4* is sufficient to recapitulate Zn distribution typical for *A. halleri* in the roots of the non-hyperaccumulator *A. thaliana*. Roots of *AhHMA4*-transformed *A. thaliana* also contained increased transcript levels of the Zn deficiency response genes *ZIP4* and *IRT3* (Fig. 4b), in analogy with wild-type *A. halleri* (see Fig. 1e, f). These results further support the model that in roots of *A. halleri*, the high *HMA4*-dependent Zn flux into the xylem depletes symplastic Zn pools, thereby triggering the upregulation of Zn deficiency response genes in the roots[4].

A. thaliana AhHMA4 transformants grown in media supplemented with toxic concentrations of 150 µM Zn or 40 µM Cd developed enhanced leaf chlorosis and smaller rosettes, which are signs of Zn and Cd hypersensitivity of the shoots (Fig. 4c, Supplementary Fig. 11). When cultivated in 5 µM Zn, *AhHMA4* transformants were healthy and accumulated slightly higher Zn concentrations than non-transgenic plants (1.16 ± 0.07 fold, mean ± s.e.m., $n = 4$ independent experiments, $P < 0.05$; data not shown). These results suggest a more efficient transfer of metals from roots to leaves in *AhHMA4* transformants compared to non-transgenic *A. thaliana*. The metal sensitivity of shoots of *A. thaliana* expressing *AhHMA4* indicates that additional genes are required for metal detoxification in order to accommodate the high *HMA4*-dependent metal flux into the shoots of *A. halleri*[7,9,22].

In summary, using a series of functional criteria[23], we have demonstrated a major role for *AhHMA4* in naturally selected Zn hyperaccumulation and associated Cd and Zn hypertolerance in *A. halleri*. High *HMA4* expression in *A. halleri* is specified in *cis* and amplified by gene copy number expansion. Increased expression of *HMA4* in *A. halleri* supports the enhanced Zn flux from the root symplasm into the xylem vessels necessary for shoot Zn hyperaccumulation, and acts as a physiological master switch to upregulate Zn deficiency response gene expression in roots (Supplementary Figure 1). These findings are of central importance for the development of phytoremediation and bio-fortification strategies. Taken together, our results provide evidence for previously proposed roles of *cis* regulatory diversification[24] and copy number expansion[25,26] in eukaryotic adaptation[27].

METHODS SUMMARY

Plant material. *A. halleri* (L.) O'Kane and Al-Shehbaz ssp. *halleri* (accession Langelsheim) or *A. thaliana* L. Heynhold (accession Columbia) were used in all experiments. Plants were cultivated hydroponically[4,5] or on a solid medium containing the hydroponic solution (HD plates) in plastic Petri dishes[28] (Methods).

Plant transformations. Constructs were generated by cloning of PCR products into GATEWAY-compatible binary vectors (Methods; Supplementary Methods for primer sequences). *A. thaliana* was transformed by floral dip[29]. *Agrobacterium tumefaciens*-mediated stable transformation of *A. halleri* was performed using a tissue-culture based procedure[30] (Supplementary Methods). Genomic DNA and RNA gel blot analyses were performed for the primary characterization of *A. halleri HMA4* RNAi transformants (Supplementary Methods).

Physiological characterization of plants. For the determination of zinc accumulation and transcript levels, plants were cultivated hydroponically at 5 µM $ZnSO_4$ in a controlled growth chamber for 3 weeks (Supplementary Methods). The Zn indicator Zinpyr-1 (Sigma) was used for confocal fluorescence imaging of Zn in roots of *A. halleri* and *A. thaliana* plants[16]. For the determination of metal tolerance, sequential root elongation assays and growth assays were performed in metal-supplemented hydroponic solutions and on HD plates, respectively (Methods).

BAC analysis and sequencing. Two *A. halleri* BACs (7C17, 17L07) covering the orthologous *HMA4* region of the *A. thaliana* genome and containing a total of three genomic *HMA4* copies of *A. halleri*, were isolated and completely sequenced (Methods). Gene and transposable element annotations were made on the basis of similarity searches performed using the BLASTN and BLASTX programs against the

TAIR database (http://www.arabidopsis.org) and the nonredundant database (nr, http://www.ncbi.nlm.nih.gov/BLAST/).

Expression analyses. Relative transcript levels were determined by real-time RT-PCR[4]. Histochemical GUS staining, fluorimetric quantitative GUS activity assays and *in situ* hybridisations were carried out according to standard procedures (Supplementary Methods).

REFERENCES

1. Mitchell-Olds, T. *Arabidopsis thaliana* and its wild relatives. *Trends Ecol. Evol.* **16**, 693-700 (2001).
2. Koornneef, M., Alonso-Blanco, C., & Vreugdenhil, D. Naturally occurring genetic variation in *Arabidopsis thaliana*. *Annu Rev. Plant Biol.* **55**, 141-172 (2004).
3. Baker, A. J. M., McGrath, S. P., Reeves, R. D., & Smith, J. A. C. in *Phytoremediation of Contaminated Soil and Water*, edited by N. Terry & G. S. Bañuelos (CRC Press LLC, Boca Raton, FL, 1999), pp. 85-107.
4. Talke, I. N., Hanikenne, M., & Krämer, U. Zinc-dependent global transcriptional control, transcriptional deregulation, and higher gene copy number for genes in metal homeostasis of the hyperaccumulator *Arabidopsis halleri*. *Plant Physiol.* **142**, 148-167 (2006).
5. Becher, M., Talke, I. N., Krall, L., & Krämer, U. Cross-species microarray transcript profiling reveals high constitutive expression of metal homeostasis genes in shoots of the zinc hyperaccumulator *Arabidopsis halleri*. *Plant J.* **37**, 251-268 (2004).
6. Weber, M. *et al.* Comparative microarray analysis of *Arabidopsis thaliana* and *Arabidopsis halleri* roots identifies nicotianamine synthase, a ZIP transporter and other genes as potential metal hyperaccumulation factors. *Plant J.* **37**, 269-281 (2004).
7. Dräger, D. B. *et al.* Two genes encoding *Arabidopsis halleri* MTP1 metal transport proteins co-segregate with zinc tolerance and account for high *MTP1* transcript levels. *Plant J.* **39**, 425-439 (2004).
8. Courbot, M. *et al.* A major QTL for Cd tolerance in *Arabidopsis halleri* co-localizes with *HMA4*, a gene encoding a Heavy Metal ATPase. *Plant Physiol.* **144**, 1052-1065 (2007).
9. Willems, G. *et al.* The genetic basis of zinc tolerance in the metallophyte *Arabidopsis halleri* ssp. *halleri* (Brassicaceae): An analysis of quantitative trait loci. *Genetics* **176**, 659-674 (2007).
10. Hoekstra, H. E. & Coyne, J. A. The locus of evolution: evo devo and the genetics of adaptation. *Evolution* **61**, 995-1016 (2007).
11. Axelsen, K. B. & Palmgren, M. G. Inventory of the superfamily of P-type ion pumps in Arabidopsis. *Plant Physiol.* **126**, 696-706 (2001).

12. Smith, N. A. *et al.* Total silencing by intron-spliced hairpin RNAs. *Nature* **407**, 319-320 (2000).
13. Krämer, U. *et al.* Free histidine as a metal chelator in plants that hyperaccumulate nickel. *Nature* **379**, 635-638 (1996).
14. Lasat, M. M. *et al.* Molecular physiology of zinc transport in the Zn hyperaccumulator *Thlaspi caerulescens*. *J. Exp. Bot.* **51**, 71-79. (2000).
15. Hussain, D. *et al.* P-type ATPase heavy metal transporters with roles in essential zinc homeostasis in Arabidopsis. *Plant Cell* **16**, 1327-1339 (2004).
16. Sinclair, S. A. *et al.* The use of the zinc-fluorophore, Zinpyr-1, in the study of zinc homeostasis in Arabidopsis roots. *New Phytol.* **174**, 39-45 (2007).
17. Clemens, S., Palmgren, M. G., & Krämer, U. A long way ahead: understanding and engineering plant metal accumulation. *Trends Plant Sci.* **7**, 309-315. (2002).
18. Grotz, N. *et al.* Identification of a family of zinc transporter genes from Arabidopsis that respond to zinc deficiency. *Proc. Natl. Acad. Sci. USA* **95**, 7220-7224 (1998).
19. Bert, V. *et al.* Genetic basis of Cd tolerance and hyperaccumulation in *Arabidopsis halleri*. *Plant Soil* **249**, 9-18 (2003).
20. MacNair, M. R. *et al.* Zinc tolerance and hyperaccumulation are genetically independent characters. *Proc. R. Soc. Lond. B* **266**, 2175-2179 (1999).
21. Windsor, A. J. *et al.* Partial shotgun sequencing of the *Boechera stricta* genome reveals extensive microsynteny and promoter conservation with Arabidopsis. *Plant Physiol.* **140**, 1169-1182 (2006).
22. Küpper, H., Lombi, E., Zhao, F. J., & McGrath, S. P. Cellular compartmentation of cadmium and zinc in relation to other elements in the hyperaccumulator *Arabidopsis halleri*. *Planta* **212**, 75-84 (2000).
23. Weigel, D. & Nordborg, M. Natural variation in Arabidopsis. How do we find the causal genes? *Plant Physiol.* **138**, 567-568 (2005).
24. Clark, R. M., Wagler, T. N., Quijada, P., & Doebley, J. A distant upstream enhancer at the maize domestication gene *tb1* has pleiotropic effects on plant and inflorescent architecture. *Nat. Genet.* **38**, 594-597 (2006).
25. Beckmann, J. S., Estivill, X., & Antonarakis, S. E. Copy number variants and genetic traits: closer to the resolution of phenotypic to genotypic variability. *Nat. Rev. Genet.* **8**, 639-646 (2007).
26. Sugino, R. P. & Innan, H. Selection for more of the same product as a force to enhance concerted evolution of duplicated genes. *Trends Genet.* **22**, 642-644 (2006).
27. Zhong, S., Khodursky, A., Dykhuizen, D. E., & Dean, A. M. Evolutionary genomics of ecological specialization. *Proc. Natl. Acad. Sci. USA* **101**, 11719-11724 (2004).
28. Arrivault, S., Senger, T., & Krämer, U. The Arabidopsis metal tolerance protein AtMTP3 maintains metal homeostasis by mediating Zn exclusion from the shoot under Fe deficiency and Zn oversupply. *Plant J.* **46**, 861-879 (2006).
29. Clough, S. J. & Bent, A. F. Floral dip: a simplified method for *Agrobacterium*-mediated transformation of *Arabidopsis thaliana*. *Plant J.* **16**, 735-743 (1998).
30. Chateau, S., Sangwan, R. S., & Sangwan-Norreel, B. S. Competence of *Arabidopsis thaliana* genotypes and mutants for *Agrobacterium tumefaciens*-mediated gene transfer: role of phytohormones. *J. Exp. Bot.* **51**, 1961-1968 (2000).

SUPPLEMEMTARY INFORMATION

Supplementary Information is linked to the online version of the paper at www.nature.com\nature. A figure summarising the main result of the paper is also included as Supplementary Fig. 1.

ACKNOWLEDGEMENTS

We thank D. Baurain, D. Walther, C. Galante, T. Werner and the Institute's gardeners for assistance, R. Schmidt for *A. thaliana* $35S_P$-GUS lines, I. Somssich for **pJAWOHL8**, and S. Thomine for comments on the manuscript. This work was funded by: German Research Foundation Kr1967/3-1, Heisenberg Fellowship Kr1967/4-1; German Federal Ministry of Education and Research Biofuture 0311877 and GABI-ADVANCIS 0315037A; European Union RTN "METALHOME" HPRN–CT–2002–00243, InP ‘‘PHIME’’ FOOD-CT-2006-016253 (U.K.). Further funding was from ‘Fonds spéciaux pour la Recherche, University of Liège, Belgium’ (M.H., P.M.), ‘Fonds de la Recherche Scientifique – FNRS’, Belgium (M.H.), and the Max Planck Society (D.W.).

AUTHOR CONTRIBUTIONS

I.N.T., M.H., M.J.H., A.N., U.K., P.M. and J.K. performed experiments, C.L. the BAC sequencing and assembly, M.H. assembly and BAC annotation; D.W. and J.K. provided the BAC library and filters; U.K., M.H. and I.N.T. jointly designed experiments; D.W. gave experimental advice and edited the manuscript; U.K. conceived of the study and

directed the research; U.K., M.H. and I.N.T. wrote and edited the manuscript; all authors commented on the manuscript.

AUTHOR INFORMATION

Reprints and permissions information are available at www.nature.com\reprints. BAC sequences are available online (Genbank accession numbers EU382072, EU382073). The authors declare no competing financial interests. Correspondence and requests for materials should be addressed to U.K. (ute.kraemer@bioquant.uni-heidelberg.de).

FIGURE LEGENDS

Figure 1. Characterization of *A. halleri HMA4* RNAi lines. a, *AhHMA4* transcript levels relative to *EF1α* in roots of *A. halleri* wild type (WT) and $35S_P$-*GUS* transformant controls, and four *HMA4*-RNAi lines. **b**, **c**, Zinc concentrations in shoots (**b**) and roots (**c**) of *A. halleri* (*Ah*) genotypes and *A. thaliana* Col (*At*) WT, cultivated in a hydroponic solution containing 5 µM Zn for 3 weeks (DW: dry weight). **d**, Zn localization in *A. halleri* roots. Confocal images show fluorescent Zn signals (green) and cell walls (red). Scale bars: 50 µm; pc: pericycle; arrowheads highlight fluorescent Zn signals in xylem vessels. **e**, **f**, Relative transcript levels (RTL) of *IRT3* (**e**) and *ZIP4* (**f**) plotted against relative *HMA4* transcript levels, all normalized to *EF1α*, in different genotypes. **g**, Cadmium tolerance, and **h**, zinc tolerance of *A. halleri* genotypes. Values are mean ± s.e.m, n = 4 to 6 and 12 to 18 individuals for RNAi lines and wild type, respectively (**b**, **c**, **g**, **h**), n = 3 to 4 (**a**), n = 6 to 8 (**e**, **f**). *: $P < 0.05$, **: $P < 0.01$, ***: $P < 0.001$.

Figure 2. Genomic organization and expression of *HMA4* genes in *A. halleri*. a, Diagram showing two overlapping *A. halleri* genomic BACs. Genes are represented by boxes and named by *Arabidopsis thaliana* Genome Identifier codes (blue text: regions syntenic with *A. thaliana*, green: triplicated genes). Triangles indicate the direction of transcription (filled: intact genes, open: truncated or pseudogenes). Three fragments of one At2g19120 ortholog are denoted (a), (b) and (c). **b**, Relative transcript levels of *HMA4* gene copies in *A. halleri* roots, and of *AtHMA4* in *A. thaliana* roots for comparison (mean ± s.e.m., $n = 6$).

Figure 3. Levels and cell specificity of *HMA4* promoter activity in *A. halleri* (left: a, c, e, f) and *A. thaliana* (right: b, d, g, h). a, **b**, Histochemical detection of GUS activity (blue), directed by the *A. thaliana* or *A. halleri HMA4* promoters, in leaves of 5-week-old plants. **c**, **d**, Specific GUS activity in protein extracts (mean ± s.e.m., $n = 4$ to 7 independent lines; MU: 4-methylumbelliferone). Values for the CaMV 35S promoter are shown for comparison. **e** to **h,** Reporter activity in whole mounts (**e**, **g**) and transverse sections (**f**, **h**) of root tips from *AhHMA4-2$_P$-GUS* transformants representative of all *AhHMA4* promoters (Supplementary Figs. 7, 8 and 10). Tissues were stained for 18 h (**a**, **b**) or 0.5 h (**e** to **h**). The inset (**f**) shows a close-up of the vascular cylinder. Scale bars: (**a**, **b**) 5 mm, (**e**, **g**) 100 µm, (**f**) 25 µm and (**h**) 15 µm. pc: pericycle; xp: xylem parenchyma. Root anatomy differs slightly between *A. thaliana* and *A. halleri*.

Figure 4. Characterization of *A. thaliana* expressing *AhHMA4*. a, Zn localization in roots of 10-day-old seedlings. Confocal images show fluorescent Zn signals (green) and

cell walls (red). Scale bars: 25 µm; pc: pericycle, arrowheads highlight fluorescent Zn signals in xylem vessels. **b**, Relative transcript levels of *ZIP4* and *IRT3* in roots of hydroponically cultivated 5.5-week-old plants (mean ± s.e.m., n = 6). **c**, Zn and Cd toxicity in shoots of 17-day-old *AhHMA4* transformants seven days after transfer to control medium (5 µM Zn, no Cd) or medium supplemented with 150 µM Zn or 40 µM Cd.

METHODS

Plant cultivation. Plants were cultivated in a climate-controlled glasshouse at 21°C day/17°C night, constant humidity of 50%, with supplementary lighting from equal amounts of HPIT and Son-T Agro lamps (Philips) providing a photoperiod of 16 h, or in a growth chamber at 20°C day/18°C night, a humidity of 60% day/75% night, and a photoperiod of 11 h at a photon flux density 145 µmol m^{-2} s^{-1}.

Generation of constructs. All *HMA4* sequences were PCR-amplified using a proofreading polymerase (Pfu Turbo, Stratagene), and verified by sequencing after directional cloning into **pENTR/D TOPO** (Invitrogen) and again after site-directed recombination into the respective GATEWAY-compatible binary vector before plant transformation, unless indicated otherwise.

To generate the *HMA4* RNA interference construct for transformation of *A. halleri*, a fragment corresponding to bp 2,541-2,997 of the open reading frame of *AhHMA4* was amplified from *A. halleri* cDNA and subcloned into the binary vector **pJAWOHL8** (GenBank accession AF408413), generating an intron-spliced hairpin construct with antisense *AhHMA4* fragment - intron - sense *AhHMA4* fragment configuration downstream of the CaMV 35S promoter[12].

To generate promoter-reporter constructs for the transformation of *A. thaliana* and *A. halleri*, an *AtHMA4* promoter fragment of 2,625 bp was amplified from genomic DNA of *A. thaliana*. The *AhHMA4-1*, *AhHMA-2* and *AhHMA4-3* promoter fragments of 2,326, 1,311 and 1,082 bp, respectively, were amplified from *A. halleri* genomic DNA. All promoter fragments, which include promoter and 5'-UTR regions and end after the first 30 bp of the respective *HMA4* coding sequence, were subcloned into the **pMDC163** binary vector[31].

The *AhHMA4p-HMA4* construct for transformation of *A. thaliana* was generated by inserting both the *AhHMA4-1* promoter fragment and the full-length *AhHMA4* coding sequence into a promoter-less variant of the **pMDC32** vector[31] (Supplementary Methods).

Physiological characterization of plants. *A. halleri* plants were maintained in hydroponic culture[4,5] in a climate-controlled glasshouse. *A. halleri HMA4* RNAi lines and wild type control individuals were propagated vegetatively *via* rooting of shoot cuttings on sand for 5 weeks and subsequently cultivated in hydroponics for 4 to 5 weeks before initiating experimental treatments. Results for wild type controls were averaged from the following *A. halleri* individuals: (1) untransformed, (2) regenerated from tissue culture following mock transformation and (3) transformed with a cauliflower mosaic virus (CaMV) 35S promoter-*GUS-Intron* construct[32]. *A. thaliana* plants were grown from seeds in hydroponic culture[4,5] for six weeks before experimental treatments were initiated.

Metal tolerance of *A. halleri* genotypes was determined in a climate-controlled glasshouse by measuring root elongation in a slightly modified hydroponic control solution (5 µM Zn, no added Cd, 0.14 mM KH_2PO_4 to avoid precipitation at high metal

concentrations), and subsequently in the presence of sequentially increased metal concentrations, in 5-day intervals (Zn: 800 µM, 1.5 mM; Cd: 10 µM, 30 µM)[20]. Two experiments were performed for each metal.

For metal tolerance assays in *A. thaliana AhHMA4* transformants (T1 generation), 10-day-old hygromycin-resistant seedlings were transferred onto HD plates containing 5 µM $ZnSO_4$ (control), 150 µM $ZnSO_4$, or 40 µM $CdSO_4$ (and 5 µM $ZnSO_4$) and maintained in a climate-controlled growth chamber. Photographs of representative individuals were taken one week after transfer. The experiment was repeated three times, with three plates per genotype and 10 replicate seedlings per plate in each experiment.

For Zn imaging, segments of newly formed distal roots were used of *A. halleri* plants grown in a hydroponic medium containing 1 µM $ZnSO_4$. For *A. thaliana*, seedlings (T3 generation) were grown for 10 days on HD plates in a climate-controlled growth chamber and incubated in hydroponic solution with 25 µM $ZnSO_4$ for 2.5 h prior to staining. Fluorescence of the Zn-Zinpyr-1 chelate was observed using confocal laser scanning microscopy (Leica SP2, Germany) with 488 nm excitation using FITC and Texas Red filters. For *A. thaliana*, two transgenic *AhHMA4* lines showing increased *HMA4* transcript levels were analysed. For *A. halleri*, *AhHMA4* RNAi lines 4.2.1, 5.4.2 and 6.5.1 were analysed (4.2.1 is shown in Fig. 1d). Images shown are representative of the results from at least 6 wild type plants and 6 transgenic plants.

Real-time RT-PCR analysis. Preparation of total DNase-treated RNA, synthesis of cDNA, primer design and sequences, quality control and data analysis were as described[4]. Values shown in Fig. 1a are averages from three to four independent biological experiments, values shown in Figs. 1e-f, 2b and 4b are averages from six to

eight technical replicates from one experiment representative of a total of three independent biological experiments.

BAC analysis and sequencing. A BAC library was constructed in the **pIndigoBAC-536** vector using *Hin*dIII-digested total genomic DNA of 8 individuals from *A. halleri* ssp. *halleri*, accessions Roderbacherbrunn and Stutenkamm (Germany) (Keygene, The Netherlands), and screened with an *HMA4* probe[4] as described[33]. A total of 18 positive BAC clones were obtained. A combination of Southern Blots and restriction pattern analyses, together with BAC end sequencing, demonstrated that two BACs (7C17, 17L07) covered all of a total of three genomic *HMA4* copies of *A. halleri*, and the orthologous *HMA4* region of the *A. thaliana* genome.

For complete sequencing, BAC 7C17 and 17L07 subclone libraries were prepared with an average insert size of 5 to 10 kb, and a total of 1,152 positive clones for each BAC were end-sequenced to a 13-fold coverage as described[34]. Sequence reads were base-called using the LifeTrace software[35] and assembled into contigs with the PHRAP and CONSED software packages (http://www.phrap.org[36]). Remaining gaps and ambiguously assembled regions were closed and polished by primer walking and PCR with oligonucleotides designed based on the flanking sequences.

Comparative genomic sequence analyses were done with the GenomeVISTA software (http://genome.lbl.gov/vista/index.shtml[37,38]) to identify syntenic regions.

Statistics. All data evaluation and statistics were done using Microsoft Excel. Statistical analysis of data from *A. halleri HMA4* RNAi lines was performed by multiple comparisons based on analysis of variance.

31. Curtis, M. D. & Grossniklaus, U. A gateway cloning vector set for high-throughput functional analysis of genes in planta. *Plant Physiol.* **133**, 462-469 (2003).

32. Vancanneyt, G. *et al.* Construction of an intron-containing marker gene: splicing of the intron in transgenic plants and its use in monitoring early events in *Agrobacterium*-mediated plant transformation. *Mol. Gen. Genet.* **220**, 245-250 (1990).
33. Benderoth, M. *et al.* Positive selection driving diversification in plant secondary metabolism. *Proc. Natl. Acad. Sci. USA* **103**, 9118-9123 (2006).
34. Eppinger, M. *et al.* Who ate whom? Adaptive Helicobacter genomic changes that accompanied a host jump from early humans to large felines. *PLoS Genet.* **2**, e120 (2006).
35. Walther, D., Bartha, G., & Morris, M. Basecalling with LifeTrace. *Genome Res.* **11**, 875-888 (2001).
36. Gordon, D., Abajian, C., & Green, P. Consed: a graphical tool for sequence finishing. *Genome Res.* **8**, 195-202 (1998).
37. Bray, N., Dubchak, I., & Pachter, L. AVID: A global alignment program. *Genome Res.* **13**, 97-102 (2003).
38. Couronne, O. *et al.* Strategies and tools for whole-genome alignments. *Genome Res.* **13**, 73-80 (2003).

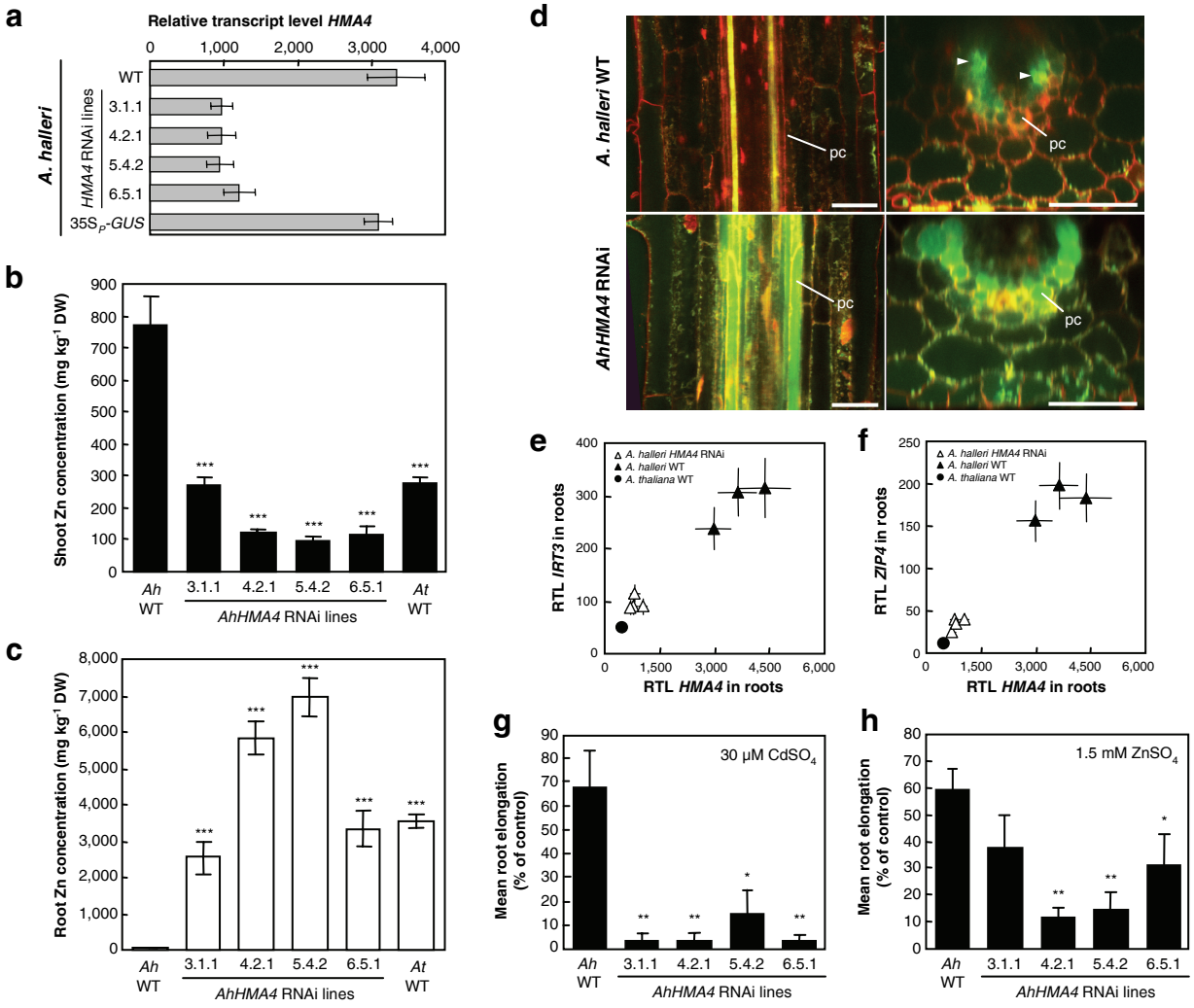
a
Relative transcript level HMA4
0
1,000
2,000
3,000
4,000
A. halleri
HMA4 RNAi lines
WT
3.1.1
4.2.1
5.4.2
6.5.1
35S$_P$-GUS
b
Shoot Zn concentration (mg kg^{-1} DW)
900
800
700
600
500
400
300
200
100
0
***
Ah WT
3.1.1
4.2.1
5.4.2
6.5.1
At WT
AhHMA4 RNAi lines
c
Root Zn concentration (mg kg^{-1} DW)
8,000
7,000
6,000
5,000
4,000
3,000
2,000
1,000
0
***
Ah WT
3.1.1
4.2.1
5.4.2
6.5.1
At WT
AhHMA4 RNAi lines
d
A. halleri WT
AhHMA4 RNAi
pc
e
RTL IRT3 in roots
400
300
200
100
0
A. halleri HMA4 RNAi
A. halleri WT
A. thaliana WT
0
1,500
3,000
4,500
6,000
RTL HMA4 in roots
f
RTL ZIP4 in roots
250
200
150
100
50
0
A. halleri HMA4 RNAi
A. halleri WT
A. thaliana WT
0
1,500
3,000
4,500
6,000
RTL HMA4 in roots
g
Mean root elongation (% of control)
90
80
70
60
50
40
30
20
10
0
30 µM CdSO$_4$
**
*
Ah WT
3.1.1
4.2.1
5.4.2
6.5.1
AhHMA4 RNAi lines
h
Mean root elongation (% of control)
80
70
60
50
40
30
20
10
0
1.5 mM ZnSO$_4$
**
*
Ah WT
3.1.1
4.2.1
5.4.2
6.5.1
AhHMA4 RNAi lines

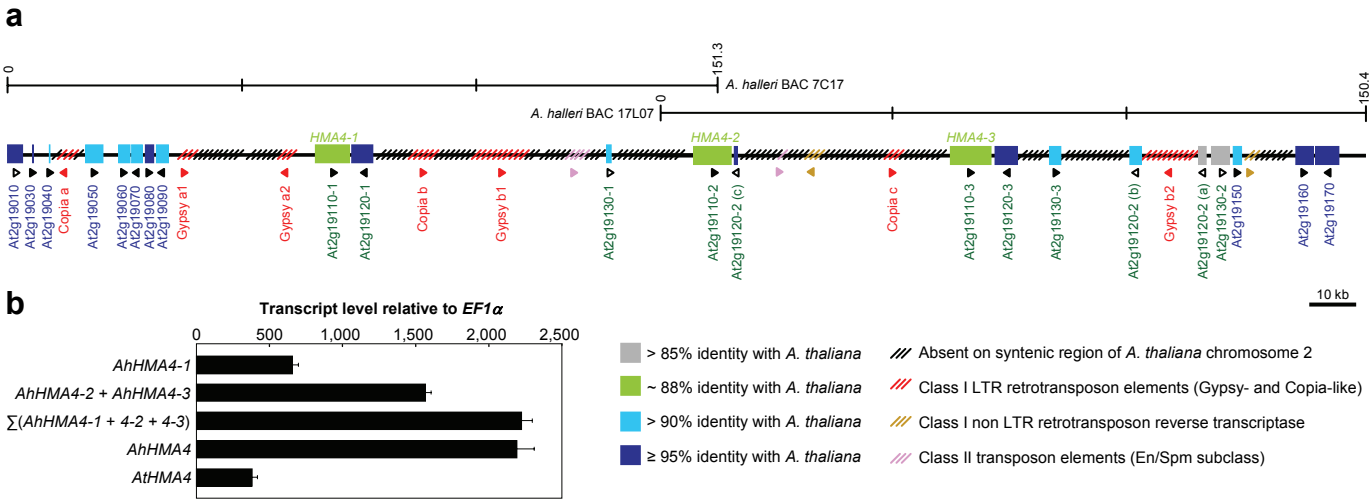
a
0
151.3
A. halleri BAC 7C17
0
150.4
A. halleri BAC 17L07
HMA4-1
HMA4-2
HMA4-3
At2g19010
At2g19030
At2g19040
Copia a
At2g19050
At2g19060
At2g19070
At2g19080
At2g19090
Gypsy a1
Gypsy a2
At2g19110-1
At2g19120-1
Copia b
Gypsy b1
At2g19130-1
At2g19110-2
At2g19120-2 (c)
Copia c
At2g19110-3
At2g19120-3
At2g19130-3
At2g19120-2 (b)
Gypsy b2
At2g19120-2 (a)
At2g19130-2
At2g19150
At2g19160
At2g19170
10 kb

b
Transcript level relative to EF1α
0
500
1,000
1,500
2,000
2,500
AhHMA4-1
AhHMA4-2 + AhHMA4-3
∑(AhHMA4-1 + 4-2 + 4-3)
AhHMA4
AtHMA4

> 85% identity with A. thaliana
~ 88% identity with A. thaliana
> 90% identity with A. thaliana
≥ 95% identity with A. thaliana
Absent on syntenic region of A. thaliana chromosome 2
Class I LTR retrotransposon elements (Gypsy- and Copia-like)
Class I non LTR retrotransposon reverse transcriptase
Class II transposon elements (En/Spm subclass)

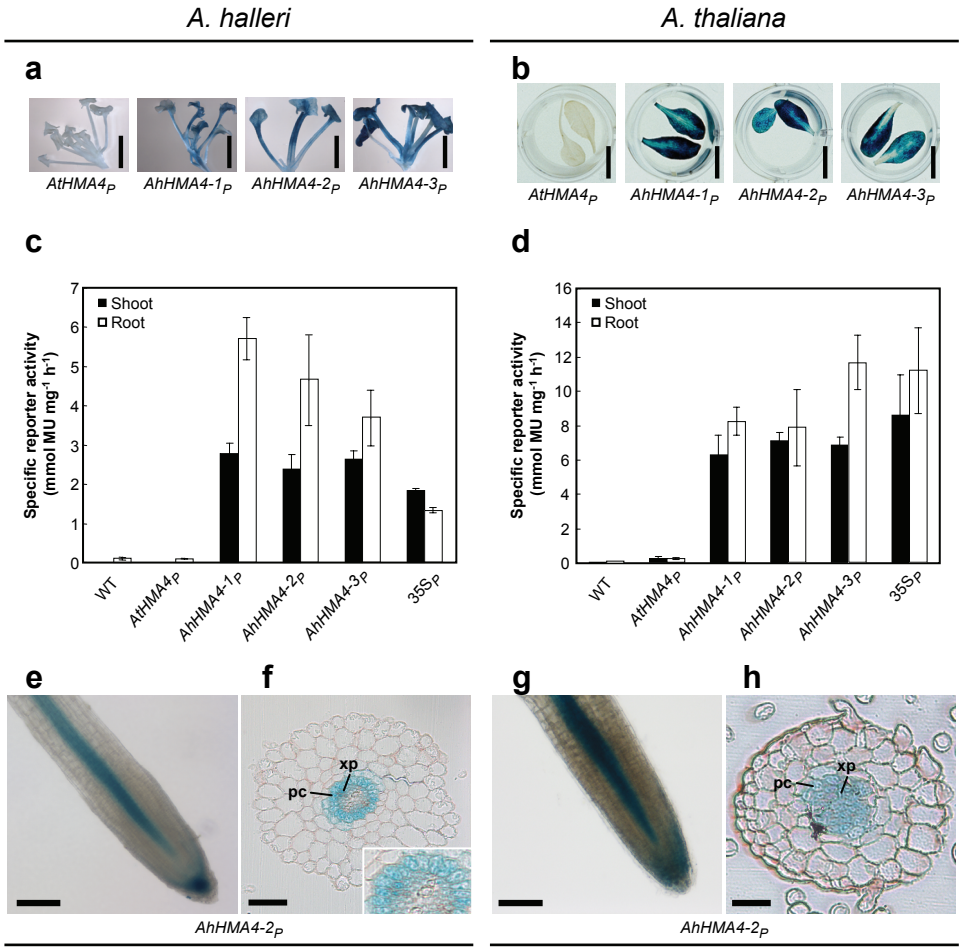
A. halleri
A. thaliana
a
b
AtHMA4P
AhHMA4-1P
AhHMA4-2P
AhHMA4-3P
c
d
Shoot
Root
Specific reporter activity (mmol MU mg-1 h-1)
WT
AtHMA4P
AhHMA4-1P
AhHMA4-2P
AhHMA4-3P
35SP
e
f
g
h
xp
pc
AhHMA4-2P
AhHMA4-2P

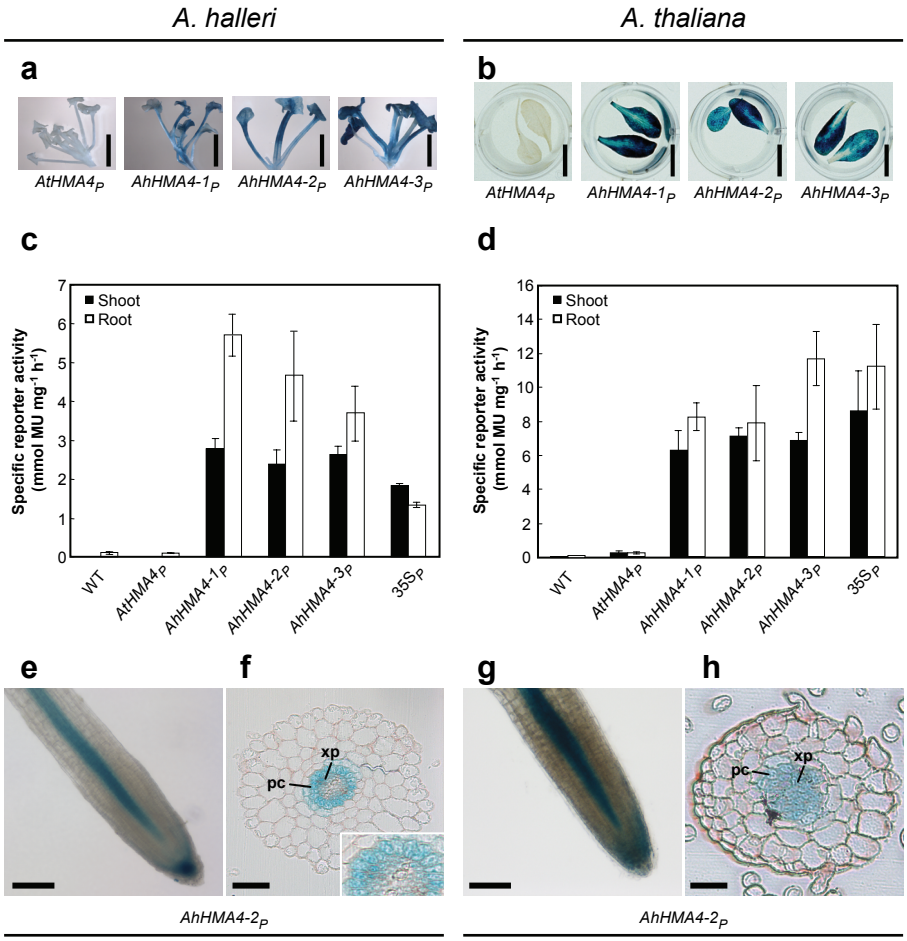
A. halleri
A. thaliana
a
b
AtHMA4P
AhHMA4-1P
AhHMA4-2P
AhHMA4-3P
c
d
Specific reporter activity (mmol MU mg-1 h-1)
Shoot
Root
WT
AtHMA4P
AhHMA4-1P
AhHMA4-2P
AhHMA4-3P
35SP
e
f
g
h
xp
pc
AhHMA4-2P

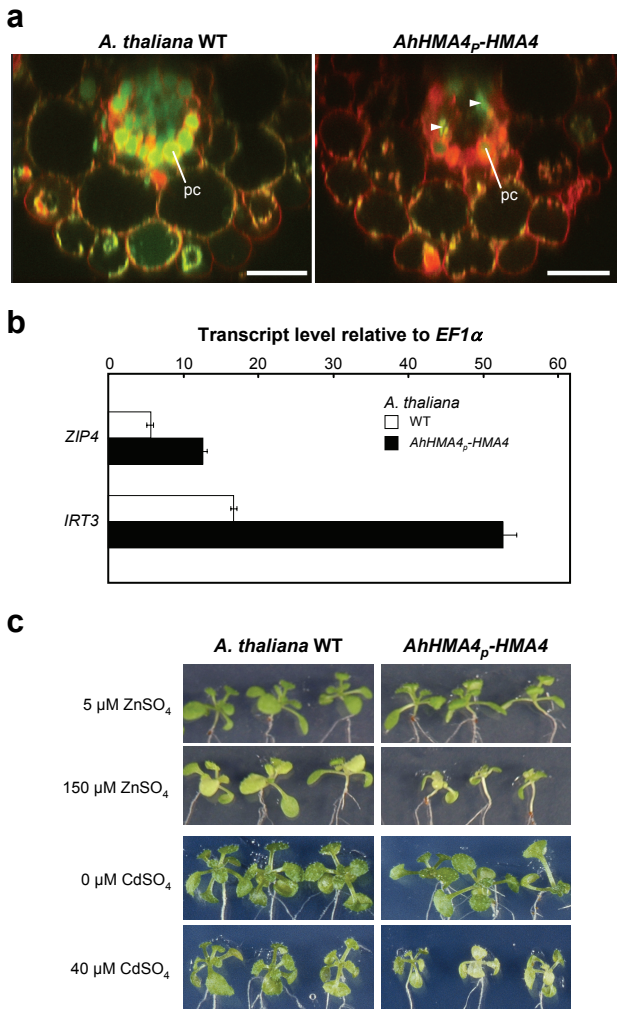
a
A. thaliana WT
AhHMA4p-HMA4
pc
pc
b
Transcript level relative to EF1α
0
10
20
30
40
50
60
A. thaliana
WT
AhHMA4p-HMA4
ZIP4
IRT3
c
A. thaliana WT
AhHMA4p-HMA4
5 μM ZnSO4
150 μM ZnSO4
0 μM CdSO4
40 μM CdSO4

Supplementary Information

Evolution of metal hyperaccumulation required *cis*-regulatory changes and triplication of *HMA4*

Marc Hanikenne, Ina N. Talke, Michael J. Haydon, Christa Lanz, Andrea Nolte, Patrick Motte, Jürgen Kroymann, Detlef Weigel, Ute Krämer[¶]

[¶]To whom correspondence should be addressed.

E-mail: ute.kraemer@bioquant.uni-heidelberg.de

This pdf file includes

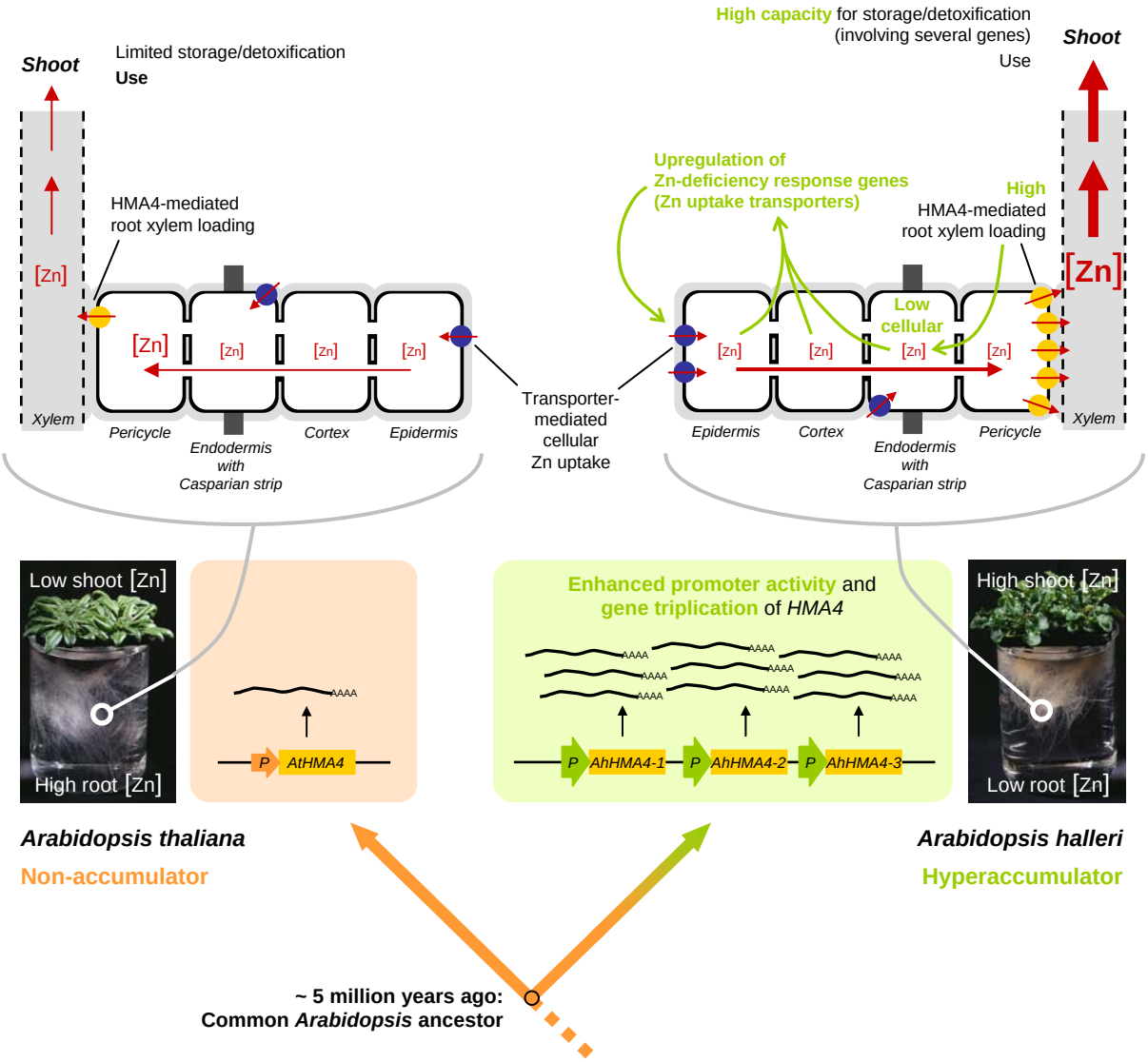

Supplementary Figure 1. Evolution of metal hyperaccumulation required *cis*-regulatory changes and triplication of *HMA4*. In the natural metal hyperaccumulator *Arabidopsis halleri*, both Zn hyperaccumulation and full Cd and Zn hypertolerance depend on high expression levels of *AhHMA4* (Fig. 1). The high expression of *A. halleri HMA4*[4] is determined by a combination of copy number expansion and enhanced promoter activity specified in *cis* of a total of three functional gene copies, in comparison to the single *HMA4* gene of the non-accumulating sister species *A. thaliana* (Figs. 2, 3). The genomic changes altering *AhHMA4* expression were thus of key importance in the evolution of both metal hyperaccumulation and hypertolerance in *A. halleri*.

The *HMA4* genes of both *A. halleri* and *A. thaliana* encode plasma membrane[8,39] Zn/Cd-transporting P_{1B}-ATPases and are expressed in the root pericycle and xylem parenchyma cells adjacent to the xylem in the vasculature (Figs 3e-h, Supplementary Fig. 10)[15]. High expression of *HMA4* drives high Zn flux into the apoplastic xylem of the root (Figs. 1d, 4a), from where solutes can passively move into the shoot xylem with the transpiration stream. By reducing root symplastic Zn, high *HMA4* expression triggers increased expression of several Zn-deficiency response genes in the roots (Figs 1e-f, 4b). Thus, *HMA4* acts as a physiological master switch in metal hyperaccumulation. The metal sensitivity of shoots of *A. thaliana* expressing *AhHMA4* (Fig. 4c) highlights that *A. halleri* possesses additional cellular metal detoxification systems that operate in the leaves to accommodate the high *HMA4*-dependent metal flux into the shoot[7,9]. In the upper section, the apoplast is coloured in grey, the intracellular symplast in white.

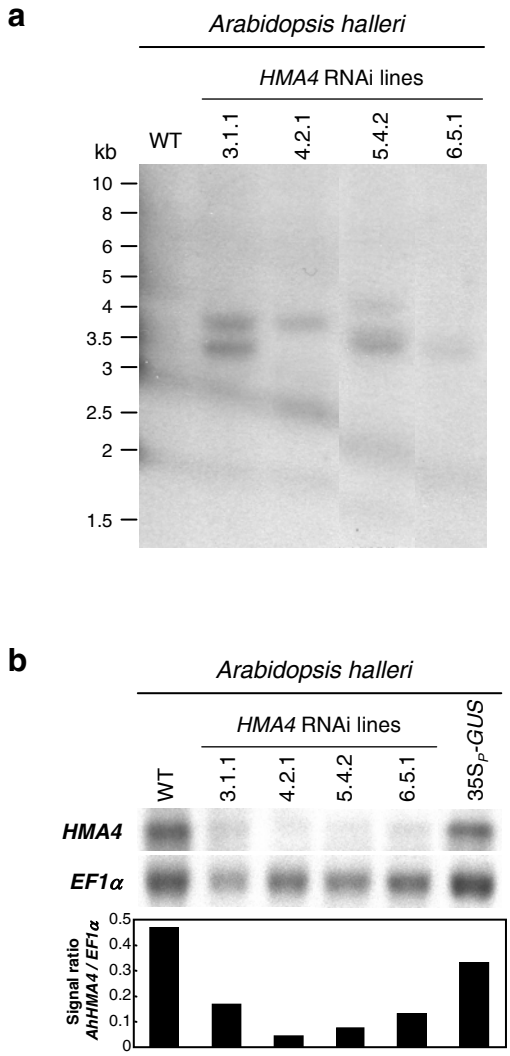

Supplementary Figure 2. Primary characterization of *A. halleri HMA4* RNAi lines. **a**, Genomic DNA gel blot analysis. Genomic DNA was digested with *Hin*dIII, which cuts once within the T-DNA approximately 1.2 kb upstream of the right border, directly upstream of the sequence used as a probe. Estimated sizes of the detected bands in the *AhHMA4* RNAi lines were: 3.3 and 3.7 kb (3.1.1), 2.6 and 3.3 kb (4.2.1), 3.5 and 4 kb (5.4.2), 3.3 kb (6.5.1), with no specific signals below 2.5 kb. Note that cross-hybridization of the probe with the size marker at 3.0 and 2.0 kb caused an unspecific diagonal background smear. **b**, RNA gel blot analysis of *HMA4* and *EF1α* mRNA levels in roots of four *A. halleri HMA4* RNAi lines, wild type (WT) and $35S_P$-*GUS* transformant controls, and quantification of the *HMA4* signal relative to the respective *EF1α* signal of the blot shown. Transcript levels of *AhHMA2* and *AhHMA3*, which are the only genes displaying significant sequence homology to *AhHMA4*, were unchanged in *HMA4* RNAi lines when compared to controls, as determined by real-time RT-PCR (data not shown).

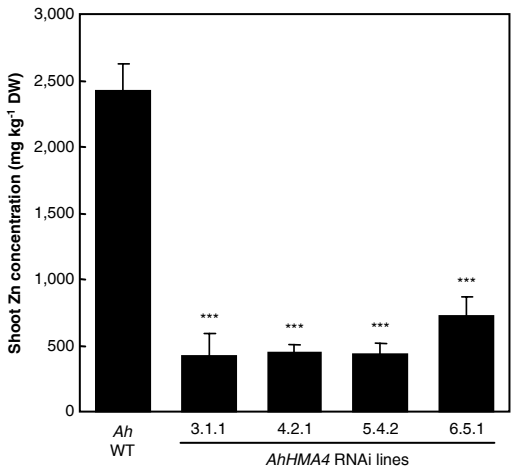

Supplementary Figure 3. Zinc accumulation in *A. halleri HMA4* RNAi lines supplied with high zinc concentrations. Zinc (Zn) concentrations in shoots of *A. halleri* (*Ah*) genotypes cultivated in a hydroponic solution containing 100 µM $ZnSO_4$ for 1 week. Values are mean ± standard error (s.e.m.), $n = 4$ for RNAi lines and 9 for *Ah* wild type. *: $P < 0.05$, **: $P < 0.01$, ***: $P < 0.001$.

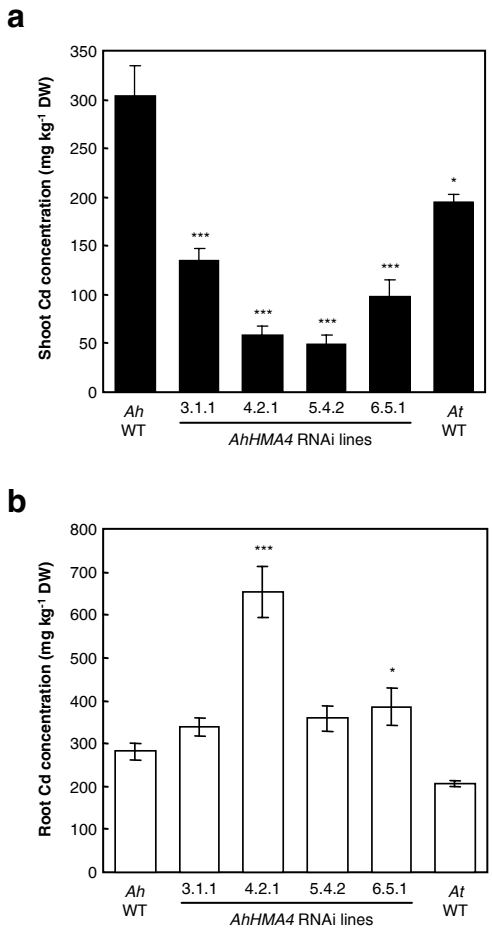

Supplementary Figure 4. Cadmium accumulation in *A. halleri HMA4* RNAi lines. Cadmium (Cd) concentrations in shoots (**a**) and roots (**b**) of *A. halleri* (*Ah*) genotypes and *A. thaliana* Col (*At*) wild type (WT), cultivated in a hydroponic solution supplemented with 5 µM $CdSO_4$ for 1 week. The hydroponic solution contained 5 µM Zn and was exchanged once during the Cd treatment, 3 d before plants were harvested. Values are mean ± s.e.m., $n = 4$ to 6 individuals for RNAi lines and *At* and 17 for *Ah* wild type. Note that in experiments with Cd treatment, all *A. halleri HMA4* RNAi lines displayed statistically significant altered partitioning of Zn to shoots and roots, when compared to wild type *A. halleri* (similar to Figures 1b and 1c, Supplementary Figure 3). Although quantitatively less pronounced and not consistent across all lines and experiments, we observed a tendency towards increased concentrations of Cu, Mn and Fe only in Cd-supplemented RNAi lines, which was more noticeable in roots than in shoots. This underscores the enhanced toxicity of Cd in *HMA4* RNAi lines and thus the role of *HMA4* in Cd hypertolerance in wild-type *A. halleri* (Figure 1g). *: $P < 0.05$, **: $P < 0.01$, ***: $P < 0.001$.

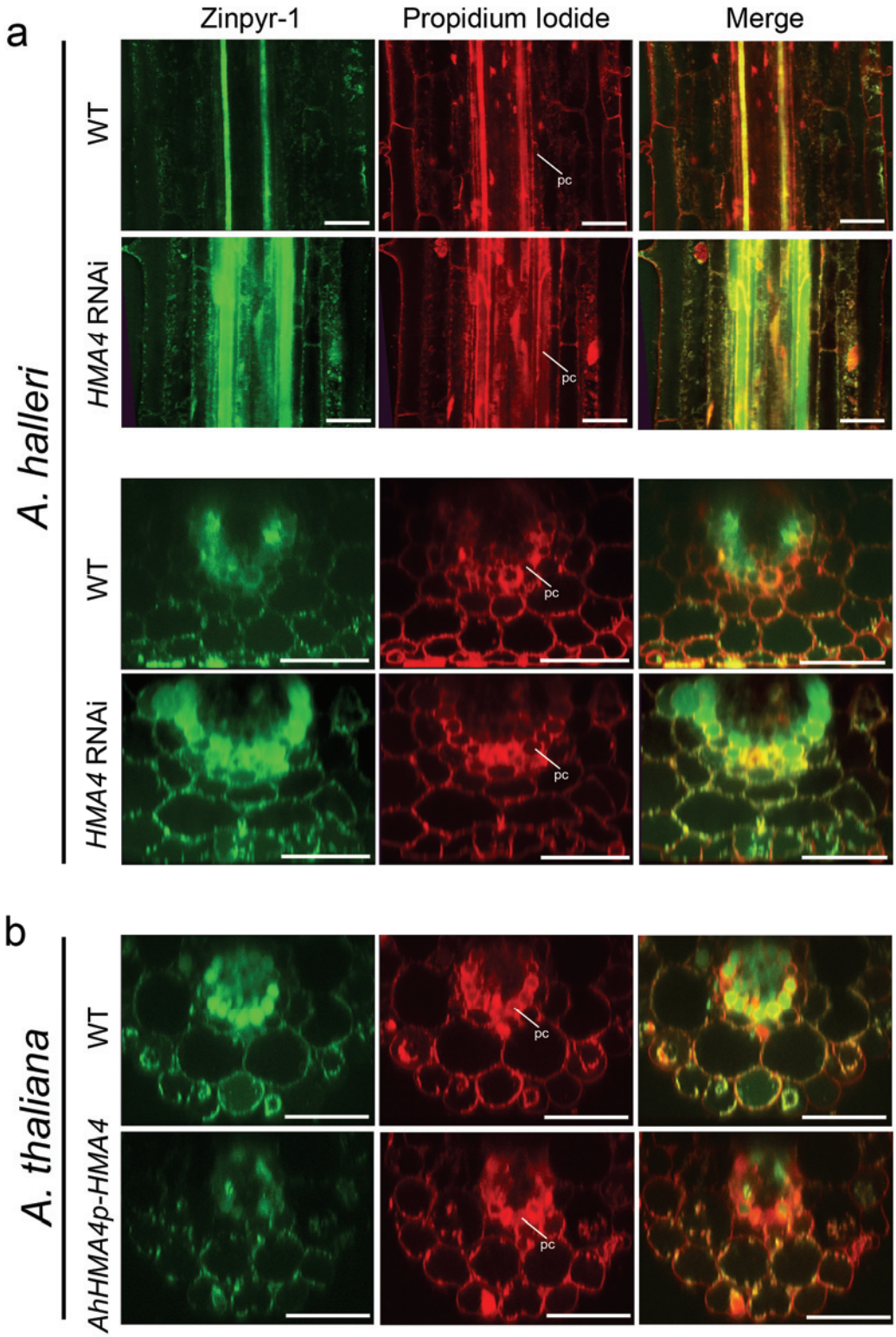

Supplementary Figure 5. Fluorescence imaging of Zn in roots of *A. halleri HMA4* RNAi and *A. thaliana AhHMA4* lines with Zinpyr-1. Confocal images of fluorescent Zn signals using Zinpyr-1 as a Zn indicator (green, left), the cell wall marker, propidium iodide (red, middle) and merged images (right) in intact roots of (**a**) *A. halleri* wild-type (WT) and a representative *HMA4* RNAi line and (**b**) *A. thaliana* wild-type (WT) and expressing *AhHMA4*. Longitudinal *xy* optical sections (**a**, top) and optical *xz* cross-sections (**a**, bottom) are shown for *A. halleri*, and cross-sections are shown for *A. thaliana* (**b**). The pericycle cell layer (pc) is indicated in propidium iodide images and represents the outer layer of the vascular cylinder. Note the higher Zinpyr-1 fluorescence in pericycle and outer cell layers in *A. halleri HMA4* RNAi (**a**) and the reduced fluorescence in these cell types in *A. thaliana* expressing *AhHMA4* (**b**), compared to WT controls. Scale bars: 50 µm.

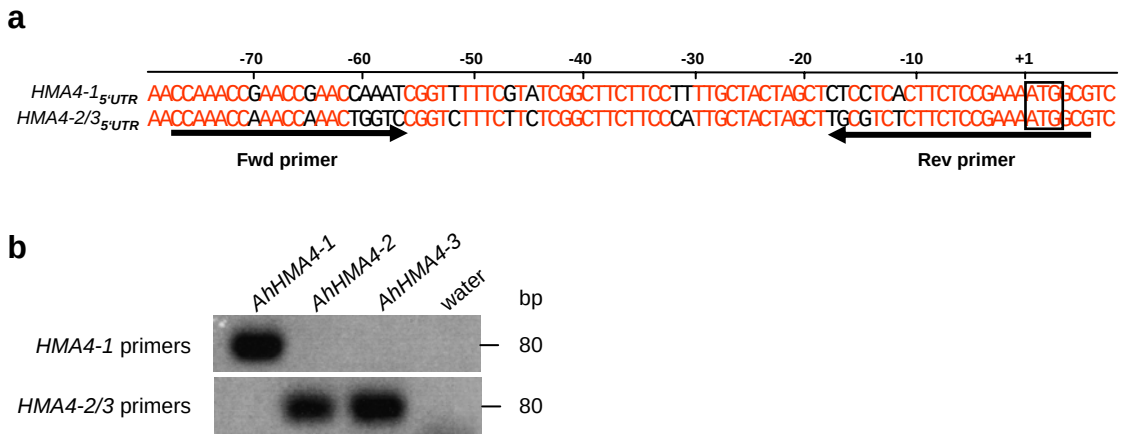

Supplementary Figure 6. **Copy-specific primer pairs for *A. halleri HMA4* genes. a**, Alignment of the proximal portions of the 5' UTRs of *HMA4-1*, *-2 and -3*. Note that the sequences of copies 2 and 3 are identical. The translational start codon is boxed, and the positions of the forward (Fwd) and reverse (Rev) primers are indicated by arrows. **b**, Specificity of primer pairs for copy 1 (*HMA4-1*) or copies 2 and 3 (*HMA4-2/3*). Plasmid DNAs, each of which contained the 5' UTR of only one of the three *HMA4* gene copies, were used as templates in PCR reactions. A very high level of identity between cDNA sequences did not allow the design of primer pairs specific for *HMA4-2* or *HMA4-3* alone.

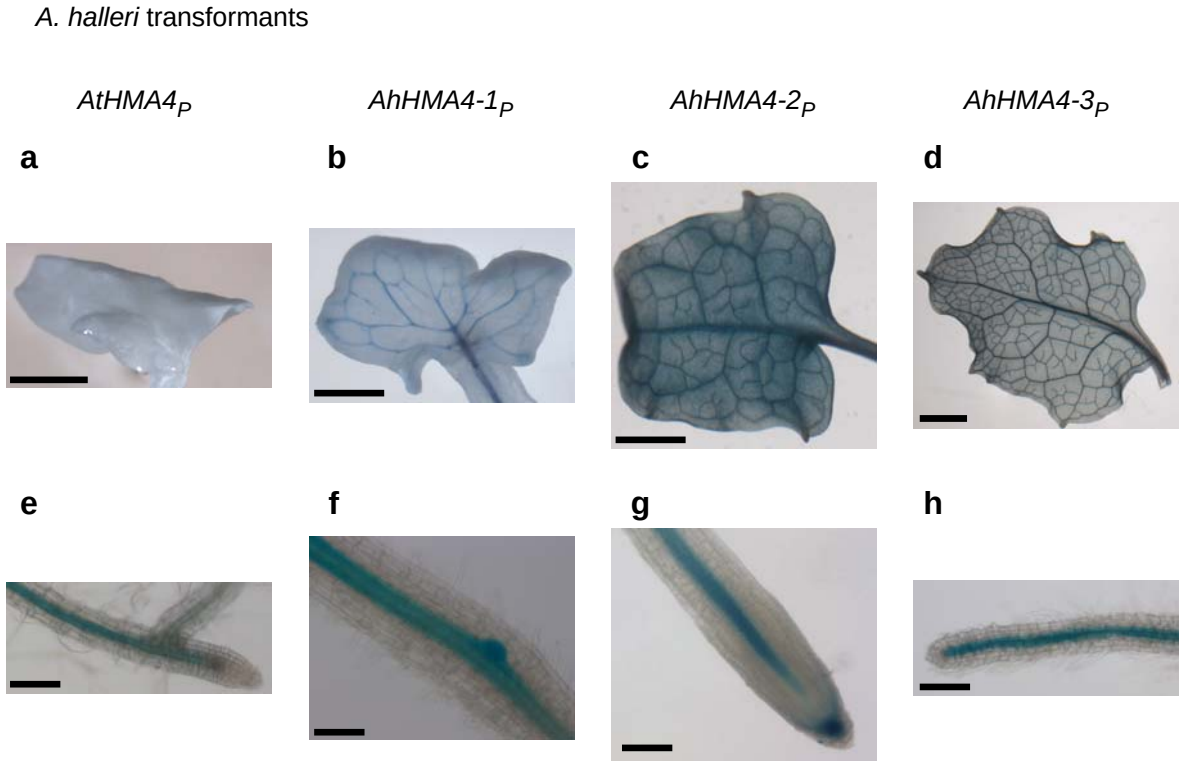

Supplementary Figure 7. **Localization of *HMA4* promoter activity in *A. halleri* reporter lines.** Histochemical detection of GUS activity (blue) in (**a** to **d**) leaves and (**e** to **h**) roots, directed by the *AtHMA4* (**a**, **e**) or the *AhHMA4* promoters (**b** to **d**, **f** to **h**). GUS staining was observed in the root tips of all *AhHMA4-2*$_P$-GUS lines and of 50% of the *AhHMA4-1*$_P$-GUS and *AhHMA4-3*$_P$-GUS lines, respectively. The picture from Fig. 3**e** is shown again here (**g**) for comparison. The duration of staining was 18 h (**a**, **e**) or 0.5 h (**b** to **d**, **f** to **h**). Scale bars: 1 mm (**a**-**d**), 200 µm (**e**, **h**) and 100 µm (**f**, **g**).

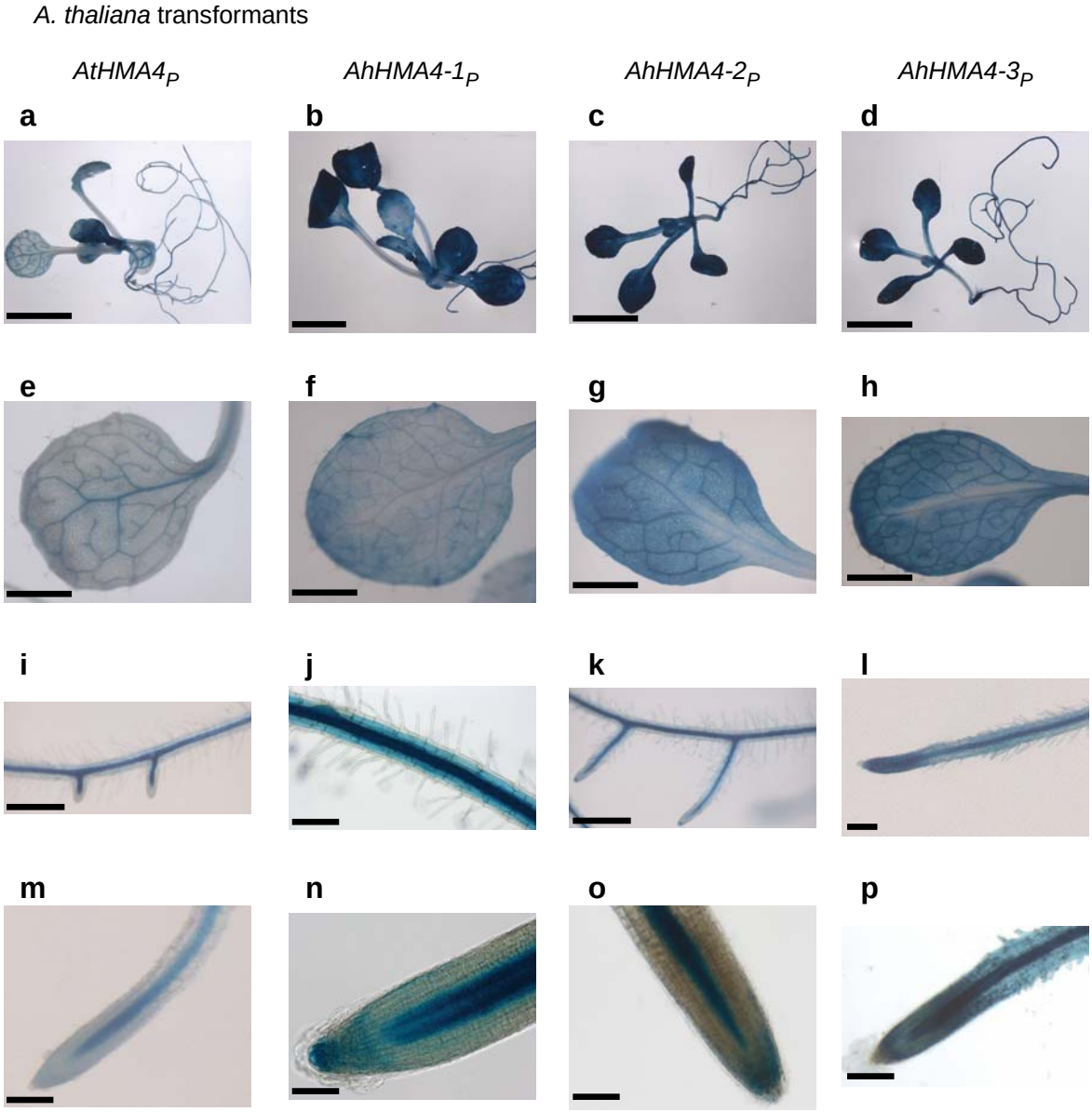

Supplementary Figure 8. **Localization of *HMA4* promoter activity in *A. thaliana* reporter lines.** GUS activity (blue) in (**a** to **d**) whole seedlings, and details of (**e** to **h**) leaves and (**i** to **p**) roots of 14-day-old seedlings, directed by the *AtHMA4* (**a**, **e**, **i**, **m**) or the *AhHMA4* promoters (**b** to **d**, **f** to **h**, **j** to **l**, **n** to **p**). The picture from Fig. 3**g** is shown again here (**o**) for comparison. The duration of staining was 18 h (**a** to **d**, **e**, **i**, **m**) or 0.5 h (**f** to **h**, **j** to **l**, **n** to **p**). Scale bars: 5 mm (**a** to **d**), 1 mm (**e** to **h**), 500 µm (**i**, **k**), 200 µm (**j**, **l**, **m**, **p**) and 100 µm (**n**, **o**). Note that (**a**) and (**e**) show staining in young seedlings, whereas Fig. 3b shows staining in rosette leaves of adult plants.

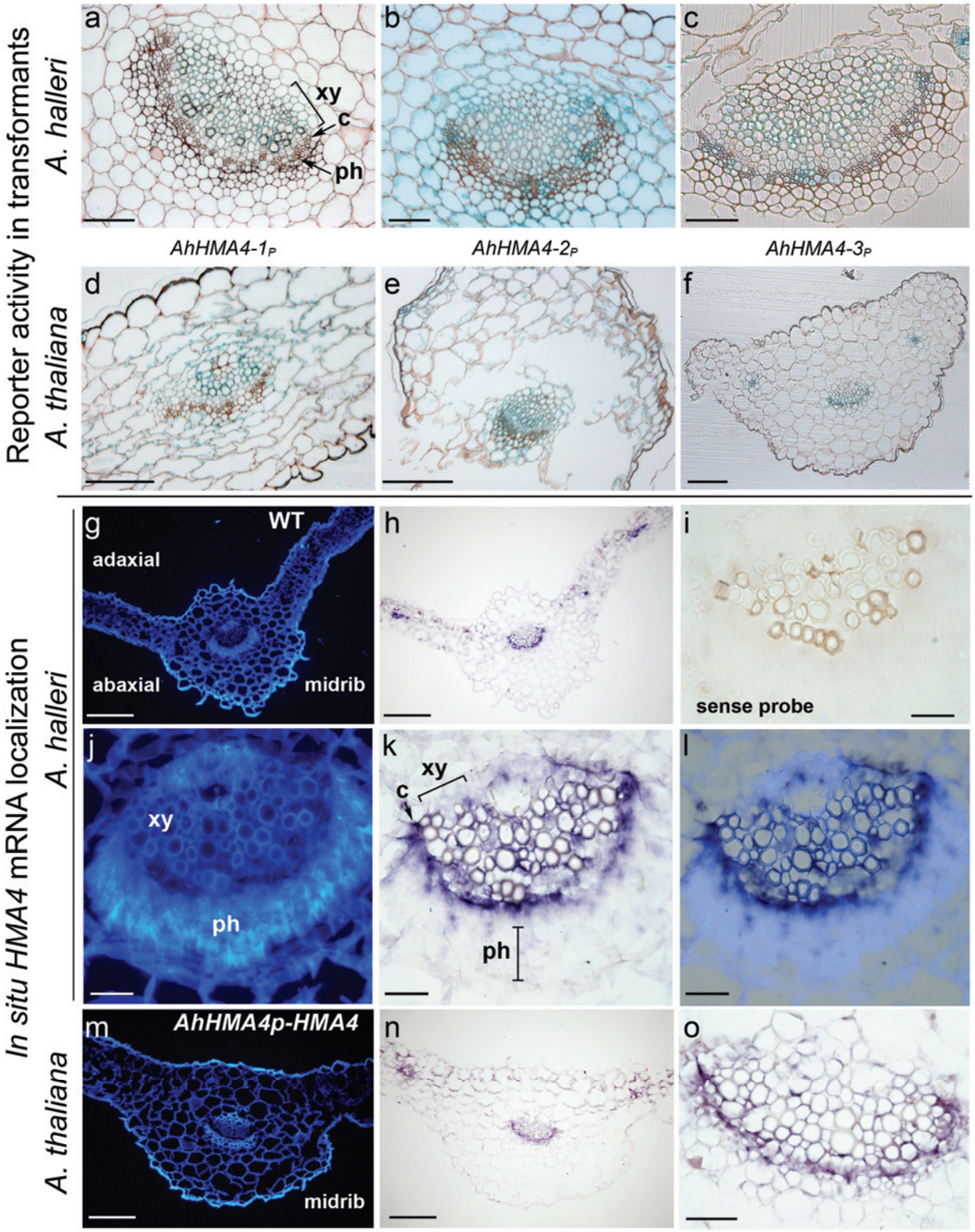

Supplementary Figure 9. **Cell specificity of *AhHMA4* expression in leaves of *A. halleri* and *A. thaliana*.** **a** to **f**, Histochemical detection of GUS activity (blue) directed by the three *A. halleri HMA4* promoters in cross-sections of petioles or leaf blades of *A. halleri* (**a** to **c**) and *A. thaliana* (**d** to **f**) lines transformed with *AhHMA4*$_P$-GUS reporter constructs (see Supplementary Figures 7 and 8). Tissues were stained for 30 min. **g** to **o**, Detection of *HMA4* transcripts by *in situ* hybridization in cross-sections of leaf blades of wild-type (WT) *A. halleri* (**g** to **l**) or transgenic *A. thaliana* expressing *AhHMA4* (**m** to **o**). (**g**, **j**, **m**) Calcofluor staining of the cell walls; (**h**, **k**, **n** and **o**) hybridization with the antisense *HMA4* probe; (**i**) control section hybridized with the sense *HMA4* probe; (**j**, **k**, **o**) central veins of panels (**g**), (**h**) and (**n**), respectively; (**l**) overlay of the pictures in panels (**j**) and (**k**). Scale bars: 100 µm (**a** to **f**, **i** to **l**, **o**) and 500 µm (**g**, **h**, **m**, **n**); c: cambium, ph: phloem, xy: xylem.

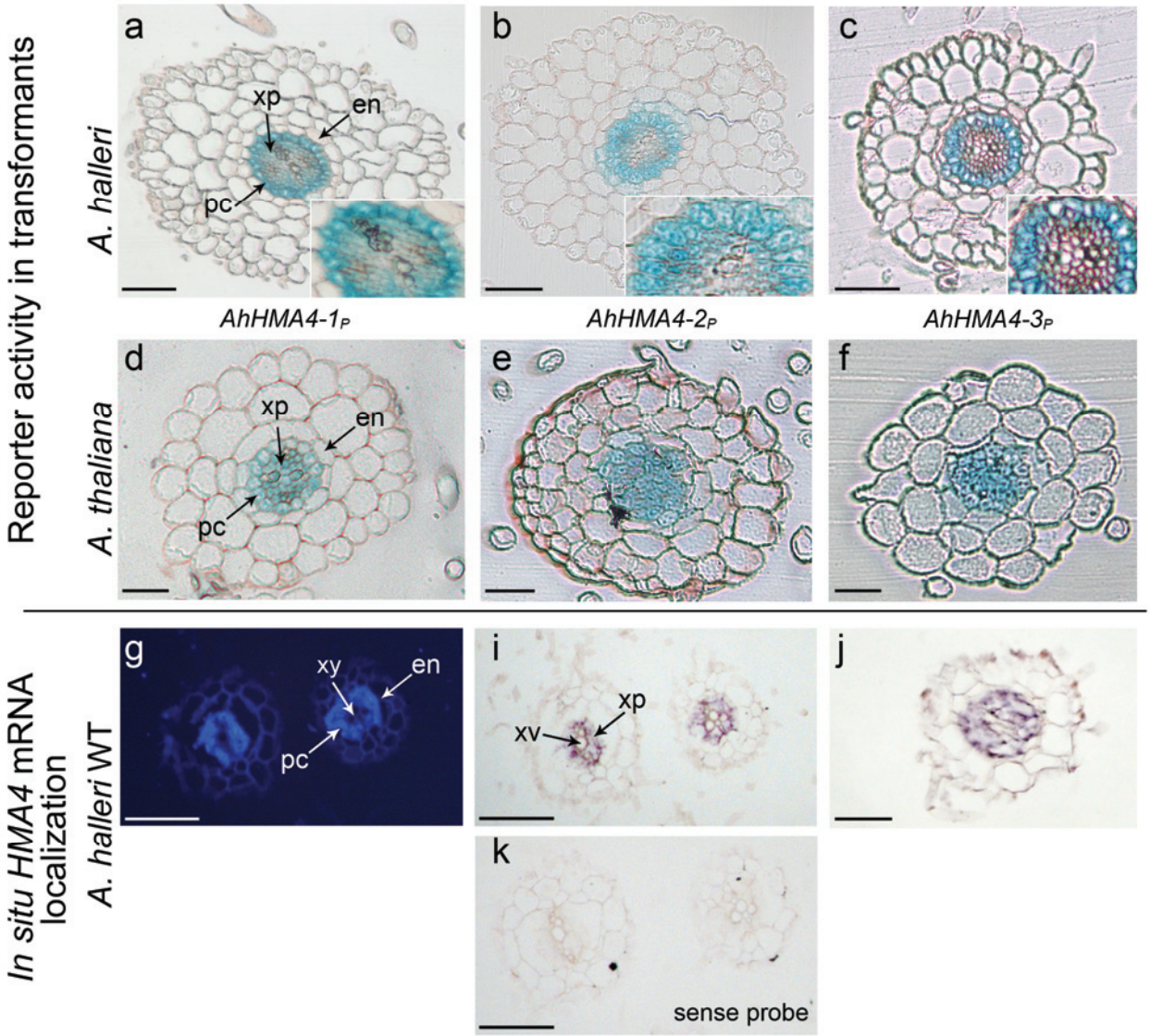

Supplementary Figure 10. **Cell specificity of *AhHMA4* expression in roots of *A. halleri* and *A. thaliana*. a** to **f**, Histochemical detection of GUS reporter activity (blue) directed by the three *A. halleri HMA4* promoters in root cross-sections of *A. halleri* (**a** to **c**) and *A. thaliana* (**d** to **f**) lines transformed with *AhHMA4*$_P$-GUS reporter constructs (see Supplementary Figures 7 and 8). Tissues were stained for 30 min. For comparison, the pictures in Fig. 3**f** and **h** are shown again here as (**b**) and (**e**), respectively. The insets (**a** to **c**) show close-ups of the vascular cylinder. **g** to **k**, Detection of *HMA4* transcripts by *in situ* hybridization in cross-sections of wild-type (WT) *A. halleri* roots. (**g**) Calcofluor staining of the cell walls; (**i**, **j**) hybridization with the antisense *HMA4* probe; (**k**) control section hybridized with the sense *HMA4* probe. Scale bars: 25 µm (**a** to **c**), 15 µm (**d** to **k**); en: endodermis, pc: pericycle, xp: xylem parenchyma, xv: xylem vessels, xy: xylem.

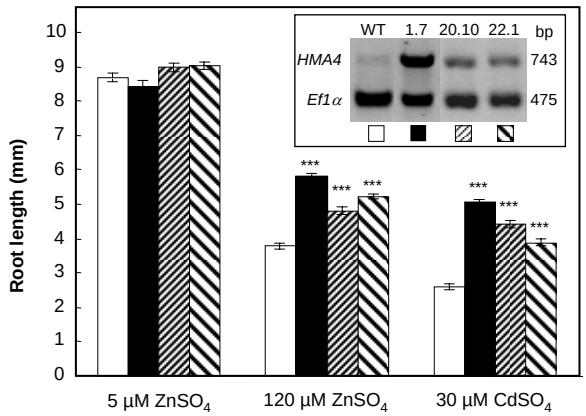

Supplementary Figure 11. Characterization of *A. thaliana* lines ectopically overexpressing *AhHMA4* under the constitutive cauliflower mosaic virus 35S promoter. Compared to wild-type *A. thaliana*, root elongation in transgenic $35S_P$-*AhHMA4 A. thaliana* lines (T3) was more tolerant to toxic concentrations of 120 µM Zn or 30 µM Cd (mean ± s.e.m., $n > 20$, ***: $P < 0.001$, compared to the wild type). The inset shows an RT-PCR analysis of *HMA4* and *EF1α* mRNA levels of plants grown in control (0 µM Cd, 5 µM Zn) media. Similar results were obtained for *A. thaliana* transformed with a $35S_P$-*AtHMA4* construct (data not shown). Shoot Zn concentrations in *A. thaliana* $35S_P$-*AhHMA4* lines were either unchanged (line 20.10) or reduced by on average 35.3% and 46.9% (lines 1.7 and 22.1, respectively) of those in wild-type plants (data not shown). This result is different from the corresponding result obtained by Verret *et al.* (2004)[39], which was based on the analysis of only a single transgenic line. Together, our results suggest that Zn tolerance in these $35S_P$-*AhHMA4 A. thaliana* lines is achieved by Zn exclusion, whereas in *A. halleri*, Zn hypertolerance is based on enhanced root-to-shoot Zn transport rates, combined with effective Zn detoxification in the leaves.

Supplementary Table 1. Pair-wise comparisons of the *AtHMA4* and the three *AhHMA4* promoters and coding sequences. Numbers given correspond to percentage identity at the nucleotide level. Comparisons of promoter sequences are based on the first 2,000 bp upstream of the translational start codon of *HMA4*.

	AtHMA4	*AhHMA4-1*	*AhHMA4-2*	*AhHMA4-3*
	Promoter sequences			
AtHMA4		73.3	49.3	47.9
AhHMA4-1	87.9		51.3	50.9
AhHMA4-2	87.9	99.2		82.1
AhHMA4-3	88	99	99.3	
	Coding sequences			

SUPPLEMENTARY METHODS

Primers. For the generation of constructs for plant transformation, the following primers were used: *AhHMA4* RNAi fragment, 5'-GGCAAAGAGCTGTTGTGAGA-3' and 5'-CACCTTCATCGCTGCAGCAAC-3';
AtHMA4 promoter, 5'-CACCACTTACCGATCGGGTATGCCATG-3' and 5'-TTTCTCTTCTTCTTTGTTTTGTAACGCC-3';
AhHMA4-1 promoter, 5'-CACCCACGGGACTGGTTATATTTCGGAAATGA-3' and 5'-TTTCTCTTCTTCTTTGTTTTGTGACGCC-3';
AhHMA4-2 and *AhHMA4-3* promoters, 5'-CACCGTGTTTGCTGGTGCTACTGTCTGA-3' and 5'-TTTCTCTTCTTCTTTGTTTTGTGACGCC-3'.
For the PCR performed to verify T-DNA integrity in *A. halleri* HMA4 RNAi lines, the fragment-specific primer 5'-CACCTTCATCGCTGCAGCAAC-3' and either of the pJAWOHL8 intron-specific primers 5'-CATCTTGACAATGAATCGTGATCGG-3' or 5'-CCGATCACGATTCATTGTCAAGATG-3' were used.
For the generation of an *AhEF1α* cDNA fragment for RNA gel blot analysis, primers 5'-TAAGGATGGTCAGACCCGTGA-3' and 5'-GAGACTCGTGGTGCATCTCAAC-3' were used.
Specific primer pairs used for expression analysis of the three gene copies of *AhHMA4* and their reaction efficiencies (arithmetic mean ± SD; $n = 40$ reactions) were as follows: *HMA4-1* 5'-CCAAACCGAACCGAACCAAAT-3' and 5'-GCCATTTTCGGAGAAGTGAGGAG-3' (1.901 ± 0.058); *HMA4-2/3* 5'-CCAAACCAAACCAAACTGGTC-3' and 5'-CCATTTTCGGAGAAGAGACGCA-3' (1.947 ± 0.073); *HMA4* 5'-CCCTCTCTCAACCTTTATGGTAACAC-3' and 5'-GCTAGTAGCAAAAGGAAGAAGCCG-3' (1.907 ± 0.056).

***Agrobacterium*-mediated transformation of *A. halleri*.** Stable transformation of *A. halleri* was achieved using *Agrobacterium tumefaciens* and a tissue culture based procedure[30]. *A. halleri* (L. O'Kane and Al-Shehbaz subsp. *halleri*, accession Langelsheim) were grown from seed for 6-7 weeks under sterile conditions on 0.5x MS[40] medium supplemented with 1% (w/v) sucrose, 0.05% (w/v) MES (2-N-morpholino ethanesulphonic acid), pH 5.7 and 0.75% (w/v) agar (Sigma Agar M). All subsequent sterile culture steps were carried out on MS medium containing 2% (w/v) sucrose, 0.05% (w/v) MES, pH 5.7 and 0.75% (w/v) agar, supplemented with phytohormones and selection agents. Sterile root fragments were pre-cultivated under callus-inducing conditions (1 mg l^{-1} 2,4-dichlorophenoxyactic acid, 0.5 mg l^{-1} kinetin) for 7 d before inoculation and co-cultivation with *Agrobacterium* for 3 d. Transformed *A. halleri* shoots were regenerated from infected root explants on shoot-inducing medium (SIM; 1 mg l^{-1} 6-benzylaminopurine, 0.5 mg l^{-1} α-naphthaleneacetic acid, 125 mg l^{-1} ticarcillin disodium/potassium clavulanate) Selection for the appropriate resistance marker was introduced after 7 d on SIM (50 mg l^{-1} kanamycin, 25 mg l^{-1} phosphinotricin, or 10 mg l^{-1} hygromycin). Shootlets with a single apical meristem were transferred onto root-inducing medium (1 mg l^{-1} indole-3-acetic acid, 125 mg l^{-1} ticarcillin disodium/potassium clavulanate), and selection for the appropriate resistance marker was maintained during root formation. For analysis of regenerated plants and experiments, plants were transferred into hydroponic culture.

Generation of the *AhHMA4p-HMA4* construct. The *AhHMA4p-HMA4* construct for transformation of *A. thaliana* was generated in four consecutive steps: (i) an *Acy*I restriction site was removed by site-directed mutagenesis from the pBluescript II KS+ (Stratagene) using primers 5'-TATTATCCCGTATTGACGC**G**GGGCAAGAGCAACTCGGTCG-3' and 5'-CGACCGAGTTGCTCTTGCCC**C**GCGTCAATACGGGATAATA-3' (mutagenic base in bold). (ii) The *AhHMA4-1* promoter including the first 30 bp of the *AhHMA4* coding sequence was amplified using primers

5’-ATATgaattc**ggcgcgcc**CACGGGACTGGTTATATTTCGGAAATGA-3’ and 5'-ATAT*gtcgac*TTTCTCTTCTTCTTTGTTTTGT*gacgcc*-3’ containing *Eco*RI (underlined), *Asc*I (bold), *Sal*I (italic) and *Acy*I (underlined italic) restriction sites and cloned into the *Eco*RI/*Sal*I sites of the mutated pBluescript II KS+. (iii) The full length *AhHMA4* cDNA[4] was amplified with primers 5’-CAGAAAAT*ggcgtc*ACAAAACAAAG-3’ and 5-ATAT*gtcgac***ttaattaa**TCAAGCACTCACATGGTGATGGTG-3’ containing *Acy*I (underlined italic), *Sal*I (italic), and *Pac*I (underlined bold) restriction sites and cloned into the *Acy*I/*Sal*I sites of the *AhHMA4-1* promoter-containing mutated pBluescript II KS+. (iv) The *AhHMA4p-HMA4* cassette was *Asc*I/*Pac*I-excised from pBluescript II KS+ and cloned into the corresponding sites of the pMDC32 binary vector from which the 35S promoter had been removed using *Apa*I and *Hin*dIII. To construct *35S$_P$-HMA4* vectors, *AhHMA4*[1] and *AtHMA4* (similar to reference[39]) were subcloned into the pMDC32 binary vector[41] for the transformation of *A. thaliana*. Homozygous *A. thaliana* lines (T3 generation) containing maximum *HMA4* transcript levels were identified based on RT-PCR.

Primary characterization of *A. halleri HMA4* RNAi transformants. Integration and integrity of the T-DNA carrying the *AhHMA4* RNAi construct into the genome of regenerated *A. halleri* plant lines was confirmed by PCR on genomic DNA[42] using a fragment-specific primer and an intron-specific primer in forward or reverse orientation (data not shown), and verified by genomic DNA gel blot analysis as described[4], using the *Hin*dIII/*Eco*RI-excised intron of pJAWOHL8 as radiolabeled probe. RNAi-mediated silencing of *HMA4* in regenerated plant lines was confirmed by RNA gel blot analysis[5], using the *Not*I/*Asc*I-excised *HMA4* fragment from pENTR/D and, subsequently, a 475-bp *AhEF1α* cDNA fragment as probes after radiolabeling. ImageJ (version 1.34s; National Institutes of Health, USA, http://rsb.info.nih.gov/ij/) was used for quantification of the *AhHMA4* and *EF1α* signals on the autoradiography films.

Analysis of gene expression and of metal accumulation in plants. For RNA extraction, root and shoot tissues were harvested separately[4], pooling material from at least three different individuals of a common genotype. Metal accumulation was determined in *AhHMA4* RNAi lines and wild type *A. halleri* and *A. thaliana* after hydroponic cultivation at 5 µM $ZnSO_4$ for 3 w, or 100 µM $ZnSO_4$ or 5 µM $CdSO_4$ for 1 w. For the analysis of elemental contents, root and shoot tissues were harvested separately from individual plants and processed and analyzed as described[4]. Results shown in Fig. 1b and c are from one experiment representative of a total of three independent biological experiments, for Supplementary Fig. 3 from one experiment and for Supplementary Fig. 4 from one experiment representative of a total of two independent biological experiments.
For transcript analysis and zinc accumulation measurements in *A. thaliana AhHMA4* transformants, seeds (T1 generation) were germinated on selective plates containing 0.5x MS medium supplemented with 20 µg mL^{-1} hygromycin for 10 d[28]. Hygromycin-resistant seedlings were transferred onto HD plates containing 5 µM Zn for one week before transfer into hydroponic culture and cultivation with 5 µM $ZnSO_4$ for 3 weeks. Tissues were harvested and pooled as described above. Two independent experiments were conducted, each with four vessels and 16 plants per genotype. In two additional experiments seedlings were harvested directly after the week of growth on HD plates containing 5 µM Zn.

Analysis of GUS reporter lines. Histochemical GUS staining was carried out as described[43] on homozygous (T3 generation) *A. thaliana* seedlings grown on 0.5x MS medium and on *A. halleri* transformants regenerated in tissue culture. Harvested tissues were incubated in staining solution for either 0.5 or 18 h, then ethanol extracted and fixed[44] before observation. For cross-sections, selected tissues were embedded in Technovit resin (Technovit 7100 and 3040, Heraeus Kulzer, Germany). Five µm thick sections were obtained using a microtome (RM 2155, Leica, Wetzlar, Germany) and counter-stained with ruthenium red before

observation with an Epi-Fluorescence Microscope Olympus BX 51 equipped with a digital camera. Ten independent transformant lines were analyzed for each construct for whole mounts, and three representative lines for microscopic sections.
Fluorimetric quantitative GUS activity assays were performed as described[28,43]. For *A. thaliana*, homozygous (T3 generation) seedlings from five independent lines for each construct were germinated and grown for 18 days on HD plates containing 5 µM $ZnSO_4$. Roots and shoots were harvested separately and pooled per plate (10 seedlings). Two T3 homozygous 35S*p-GUS* lines (1xf[45]) were included as controls. The experiment was repeated twice with two replicate plates per line. For *A. halleri* transformed with *HMA4*-promoter-*GUS* constructs, four to seven independent lines were analyzed per construct. At least two clones of each line were grown in hydroponic culture with 5 µM $ZnSO_4$ in a controlled growth chamber. For each line, root and shoot samples were collected from the individual clones and pooled. The experiment was repeated twice.

***In situ* hybridisation.** For probe synthesis, a 1,307-bp DNA fragment corresponding to the 3' end of the *AhHMA4* cDNA was amplified with primers 5'-GCGATGATGATGATGCTGTGGAC-3' and 5'-TCAAGCACTCACATGGTGATGGTG-3', and cloned into the pGEM-T easy vector (Promega, The Netherlands). Sense and antisense cRNA probes were synthesized and digoxigenin (dig)-labelled as described[46]. Plant materials were fixed in 4% (v/v) paraformaldehyde and dehydrated in a series of increasing ethanol concentrations. The ethanol was substituted for Histo-clear (VWR, Belgium) and tissues were embedded in Paraplast Plus (VWR, Belgium) before sectioning (~7 µm thickness). Hybridization of the dig-labelled RNA and immunological detection of the hybridized probe was carried out as described[46]. After counterstaining with 0.5% (w/v) Calcofluor, slides were mounted with Entellan (Merck, Germany) and observed with a Leica microscope equipped with a digital camera.

SUPPLEMENTARY NOTES

Supplementary references. Further references are listed in the printed paper.

39. Verret, F. *et al.* Overexpression of AtHMA4 enhances root-to-shoot translocation of zinc and cadmium and plant metal tolerance. *FEBS Lett.* **576**, 306-312 (2004).
40. Murashige, T. & Skoog, F. A revised medium for rapid growth and bio assays with tobacco tissue cultures. *Physiol. Plant.* **15**, 473-497 (1962).
41. Curtis, M. D. & Grossniklaus, U. A gateway cloning vector set for high-throughput functional analysis of genes in planta. *Plant Physiol.* **133**, 462-469 (2003).
42. Thomson, D. & Henry, R. Single-step protocol for preparation of plant tissue for analysis by PCR. *Biotechniques* **19**, 394-397, 400 (1995).
43. Jefferson, R. A., Kavanagh, T. A., & Bevan, M. W. GUS fusions: beta-glucuronidase as a sensitive and versatile gene fusion marker in higher plants. *EMBO J.* **6**, 3901-3907 (1987).
44. Desbrosses-Fonrouge, A. G. *et al. Arabidopsis thaliana* MTP1 is a Zn transporter in the vacuolar membrane which mediates Zn detoxification and drives leaf Zn accumulation. *FEBS Lett.* **579**, 4165-4174 (2005).
45. Schubert, D. *et al.* Silencing in Arabidopsis T-DNA transformants: the predominant role of a gene-specific RNA sensing mechanism versus position effects. *Plant Cell* **16**, 2561-2572 (2004).
46. Brewer, P. B. *et al.* In situ hybridization for mRNA detection in Arabidopsis tissue sections. *Nat Protoc* **1**, 1462-1467 (2006).